The University of Queensland

School of Information Technology and Electrical Engineering

Multi-Band Antenna for Handheld Transceivers

Bachelor of Engineering (Hons)
Electrical Engineering Thesis
2002

By

Choon Wee Khoo

1/242 Carmody Road,
St Lucia, Brisbane,
QLD 4067

15 October 2002

The Dean,
Faculty of Engineering, Physical Science and Architecture,
The University of Queensland,
St Lucia,
Brisbane QLD 4072

Dear Sir,

In accordance with the requirements for the Degree of Bachelor of Engineering (Honours), I hereby submit for your consideration the thesis entitled "Multi-Band Antenna for Handheld Transceivers".

This work was performed under the supervision of Associate Professor Marek E. Bialkowski. I declared that the work submitted in this thesis is my own, except as acknowledged in the text and footnotes, and have not been previously submitted for a degree at the university of Queensland or any other institutions.

Yours Sincerely,

Choon Wee Khoo

Acknowledgements

The completion of this thesis would not have been possible without the help and support of the following people. First and foremost I would express my appreciation and gratitude to my supervisor, Associate Professor Marek E. Bialkowski, for his guidance, supervision and encouragement throughout the course of this thesis. Also thanks to my friend, Louis, whom helped me in learning the use of FEKO.

Heartfelt thanks and appreciation must also go to my beloved girlfriend, Lau Ping Ping, who has always been very supportive throughout the year.

Last but not least, I would like to thank my parents for both financial and continuous support through these years.

Abstract

In the last few years, there has been an increasing demand for multi-band antennas. In particular, the focus has been on embedded antenna designs. With the third generation (3G) wireless communications systems going to be introduced worldwide, the demand for a handheld transceiver to support both old and new standards via a single antenna becomes compulsory. Therefore, the most immediate task for the new antennas is to operate in both the new UMTS (3G standards) frequency bands and the already established frequency bands. However, there is also a requirement on handheld transceivers to serve cellular bands and new communication technologies (e.g. WLAN and Bluetooth).

In this thesis, a new embedded antenna that operates in (four frequency bands) three major global mobile communications frequency bands including GSM900, GSM1800, UMTS and Bluetooth frequency band has been designed. The antenna is a single feed and low profile Planar Inverted-F Antenna (PIFA). It has three narrow slots etched on the same side of the patch. Using software, FEKO, simulations has been carried out to investigate the antenna's performance and characteristics. From the simulation results, it has been found that the antenna is able to operate at the desired resonant frequencies with the specific bandwidth.

Table of Contents

Chapter 1

Introduction and Overview

1.1 Introduction

The origination of wireless communications started in 1886 when Heinrich Hertz did an experiment to confirm the presence of electromagnetic waves based on James Maxwell's (1864) theoretical foundation for electromagnetic radiation. It was then in 1897, Guglielmo Marconi first establish the capabilities of wireless communications through continuous contact with ships sailing the English Channel [1]. Since then, antennas have always been evolving due to the development of wireless technologies, which has led to radio, television, mobile phone and satellite communications.

However, during the last decade, the mobile radio communication industry started to grow at a very fast rate, fuelled by new digital and RF circuit fabrication improvements, new large-scale circuit integration, and other miniaturization technologies which make portable radio equipment smaller, cheaper, and more reliable [1]. All these advancement in wireless technologies, have seen a trend of increasing mobile radio communications users along with smaller handheld transceivers especially in the cellular telephone industry. This has promoted more research into embedded antenna designs, which became very popular for use with mobile phones.

As we begin the 21st century, the growth in cellular telephone industry continues to rise throughout the world with an increase of 40% or more per year in cellular telephone subscription [1]. To date, more than 900 million people, about 15% of the world's population, pay a monthly subscription for cellular telephone service, and this figure is estimated to approach 30% of the population in the next few years. Due to this widespread growth in cellular telephone subscribers, mobile phone market has also

increase tremendously and this means the demand for mobile antennas is also on the rise. As shown in Figure 1.1, mobile handsets market has surpassed the 600 million mark in first quarter of 2002.

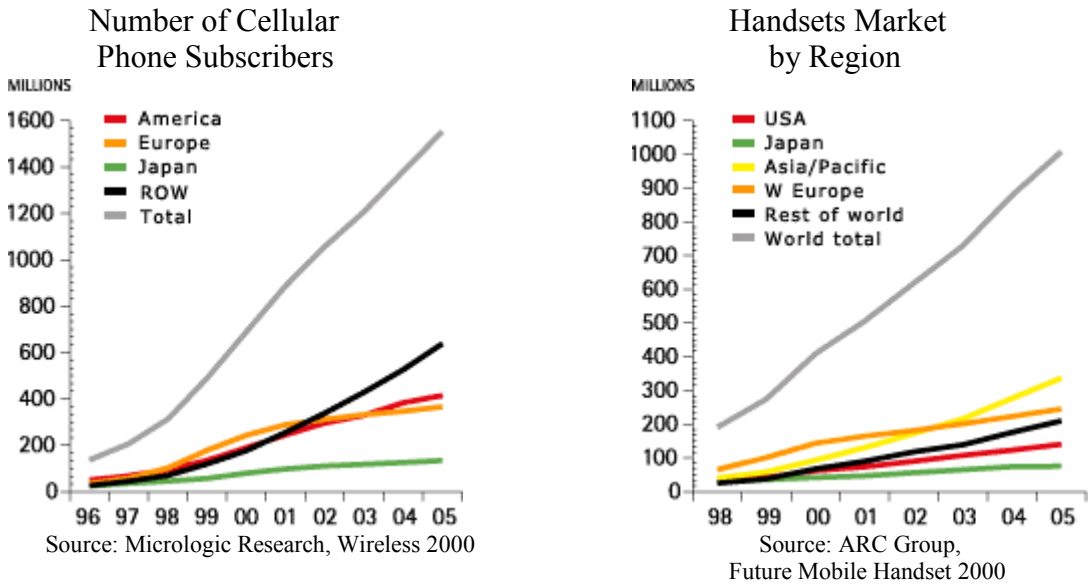

Figure 1.1: Graph showing cellular phone subscribers and handset market in the world

In the next few years, a new generation of cellular network (i.e. the third generation wireless network, 3G) will be introduced worldwide to create a single standard for all cellular phone users and provide fast connection to the Internet. With very high-speed data communications in addition to voice calls, this new 3G systems promise unparallel wireless access in ways that have never been possible before. New standards and technologies are also being introduced to allow new revolution wireless systems, which will replace fibre optic lines and copper wires. These new wireless systems such as Bluetooth and wireless local area networks (WLANs), which offer invisible wireless connections, are becoming more and more popular due to the use of low power and license free spectrums. As these new technologies start to roll out and become common to the world, more new antenna designs have to be introduced to cope with the anticipated demand.

1.2 Motivation

As mentioned earlier, in the next few years, 3G cellular network will be introduced worldwide to create a single standard for cellular phone users. Although the evolution of 3G will have a single standard implementation worldwide, the hope for that has not materialized as the worldwide user community remains split between two camps: GSM / IS-136 / PDC and CDMA, as can be seen in Figure 1.2[1]. Moreover, implementations of new 3G communications systems require expensive new base station equipment thus the installations will be slow and gradual [1]. Therefore, to have an ideal 3G implementation worldwide, multi-band antenna is required to switch between the current 2G networks and 3G networks where it is available. Besides, multi-band antenna development will also benefit the many cellular phone users who will require such function to access different communications networks in different countries.

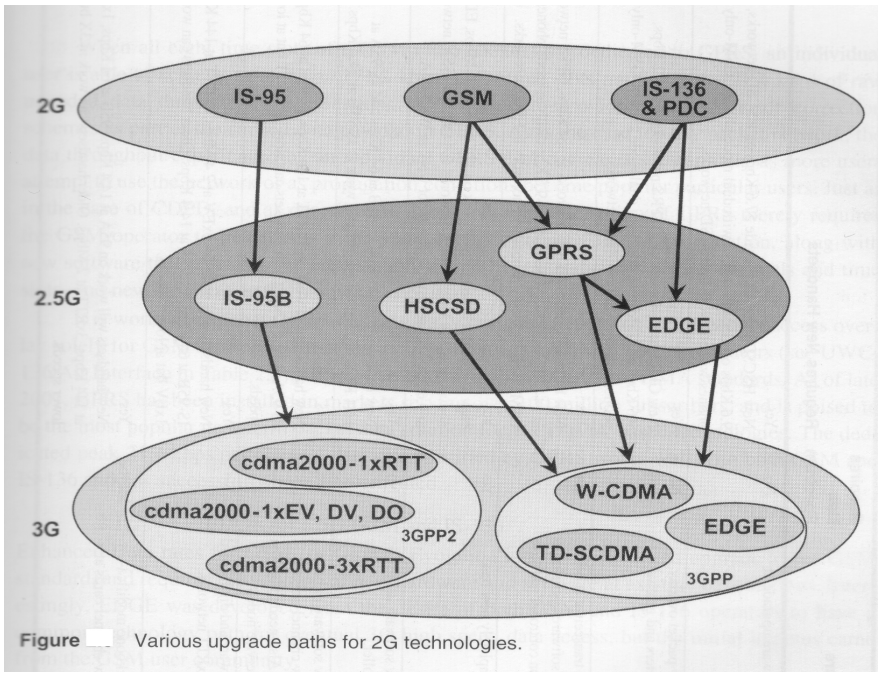

Figure 1.2: Diagram showing various paths that lead to 3G wireless communication systems

New technologies or new wireless systems such as Bluetooth and WLANs have another impact on the new antenna designs. The introduction of these new technologies has called for integration with the cellular communications systems. Despite the fact that some new antennas available in the market have already introduced the world to such integration, cellular phones with such antennas are still not commonly used. This is mainly because the implementation of such new technologies has not reach the majority users. Therefore, new antenna designs for mobile phones should include such integration before these new technologies take the world by surprise.

1.3 Aim of Thesis

With the estimated large increase of cellular telephone subscribers in years to come, the upcoming introduction of 3G wireless communications networks and new wireless systems such as Bluetooth and WLANs, there is a growing trend towards the design of multi-band antenna for use on multi purpose mobile phone. However, at present, most of the current antenna designs for mobile phone are focus mainly on the second-generation cellular network (2G), mostly offering only single band and dual band operations with a few having tri band capabilities (e.g. GSM, DCS and PCS operations). Thus the most important task now is to design new antennas that not only cover the present and future cellular frequency bands but also non-cellular frequency bands.

In this thesis, a new antenna is to be designed to operate at 4 main frequency bands (i.e. GSM900, GSM1800, UMTS and Bluetooth frequency bands). In addition, this antenna has to provide an embedded solution so as to harness the inherent advantages of the mobile phone. As a result, Planar Inverted-F Antenna (PIFA) is chosen to form the basis in this thesis due to its miniature in size, along with its abilities to have multi frequency operations shown in previous research. PIFA has also proved to be the most widely used internal antenna in commercial applications of cellular communication.

1.4 Overview of the Thesis

The Planar Inverted-F Antenna (PIFA) is a very complicated antenna. Despite extensive research and numerous reading, PIFA's design theory still remains as a mystery. However through Dr. Peter Song's advice, much of the PIFA's characteristics begin to reveal and work on the antenna design starts to fall in place. And with the steps listed below, the objectives of this thesis are finally accomplished.

i) Research on various internal multi-band antenna designs. Study and understand each antenna's characteristics. {Chapter 2}

ii) Select a suitable antenna design to form the basis for the thesis. Study and understand the antenna's theory and characteristics.
(Planar Inverted-F Antenna was the choice.) {Chapter 3}

iii) With a good understanding of PIFA, design a new antenna to perform to the requirements listed in the criteria. Simulations were being done to obtain the results on the performance of the antenna. {Chapter 4}

iv) Investigate on the characteristics of the new antenna and compare the results with the theory. {Chapter 5}

v) Assess the effects that a human has on the antenna and the health safety of the users when operating with this antenna. {Chapter 6}

Last but not least, a conclusion of the thesis is made in Chapter 7 and suggestions are made for future antenna development.

Chapter 2

Multi-Band Antenna Designs

2.1 Introduction

In the last few years, the demand and popularity of multi-band antenna has been rising. As mentioned in the previous chapter, this demand and popularity is due to the rapid advancement in wireless communications and the estimated large increase of cellular telephone subscribers in years to come. As a result, there is a surge in multi-band antenna research and development. However, having become such an integral part of our daily lives, mobile phones need to be more compact, fashionable and practical than ever before. Internal antennas offer several advantages over traditional mobile phone antennas, making them ideal for compact phones.

In this chapter, we will be looking at various multi-band antenna designs for use on handheld devices, many of which are potential candidates for use in the future mobile phone. These antennas include Microstrip antenna (MSA), Planar Inverted-F Antenna (PIFA), and some other antenna designs including the helical antenna. Most of these antennas that were developed are used to meet the demand of the increasing cellular telephones' market. Thus, the operations of these antennas are mainly focus on the major global communication networks such as GSM, DCS and PCS operations. On the other hand, there are also some internal antennas that were designed for use with the non-cellular frequency bands such as WLAN, Bluetooth and GPS, which could also be considered for implementation into the future mobile phone.

2.2 Microstrip Antenna

Microstrip antenna (MSA) is a typically low-profile antenna first introduced in the mid-1970s by R.E. Munson and J.Q. Howell [2]. However it is not until recently that MSA is suitable for use in mobile phones due to its narrow bandwidth and large size. In the paper by Y.J. Wang et al. [3], a novel and broadband semi-disc MSA (shown in Figure 2.1) is designed. Using new bandwidth enhancement and size miniaturisation methods, this small antenna is able to have a broad impedance bandwidth of 32.4% from 1.86GHz to 2.58GHz (shown in Figure 2.1), which is used to provide the antenna with multiple frequency band operation. And with this bandwidth coverage, the MSA is able to operate in the following frequency bands: DECT, IMT2000 and Bluetooth wireless system.

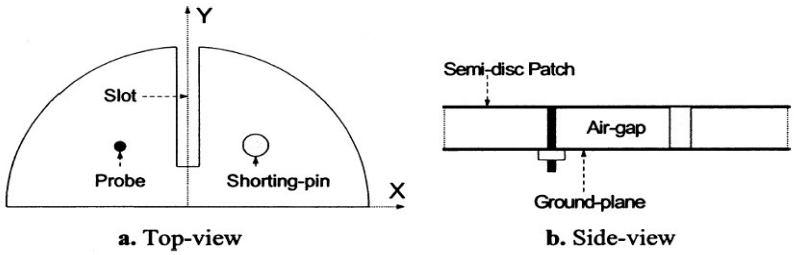

Figure 2.1: Configuration of the MSA by Wang et al. [3]

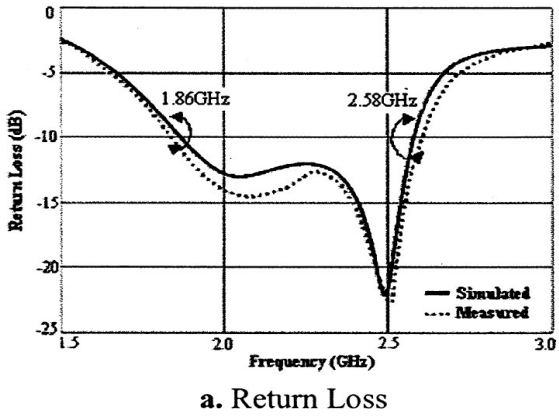

Figure 2.2: Return Loss of multi-band MSA in [3]

In another MSA design by Guo et al. [4], several other techniques including the use of high dielectric substrate, short circuit and shorting pin are used to miniaturise the antenna. On top of that, the thickness of the substrate is used to determine a wider bandwidth. However, in this case, (as shown in Figure 2.3) two antenna patches are used to provide dual frequency band operation, which in turn gave the antenna two resonant frequency bands. From the results obtained, the outer patch determines the lower frequency band while the inner patch determines the higher frequency band. The frequency band that it is designed to operate is at 900MHz and 1800MHz, so as to be implemented for mobile phone function.

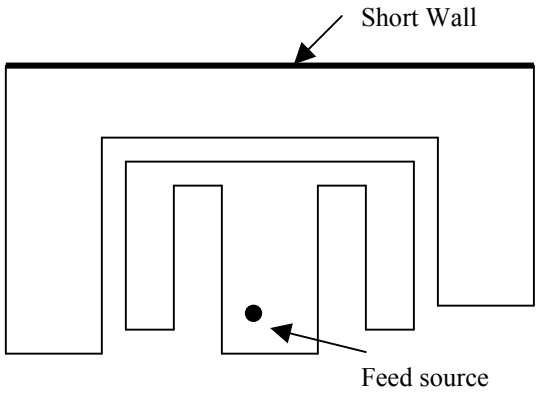

Figure 2.3: A Dual Band MSA by Guo et al. in [4]

2.3 Planar Inverted-F Antenna (PIFA)

Planar inverted-F antenna is an antenna, which is not only small in size but also has a broad bandwidth and high efficiency. Although it has a structure similar to that of a MSA, it is also well known to be a "shunt-driven inverted-L antenna – transmission line with an open end" [2]. With the advantages of the planar inverted-F antenna, it has now become very popular with mobile phone manufacturers as the demand for small mobile handsets rises.

During the mid 1990s, with evolution of the mobile phone system, demand for multi-band antenna increased with several dual band mobile phones introduced. However these mobile phones' antenna are based on wire antenna. Meanwhile with the advancement of technologies, mobile phones begin to shrink in size thus leading to an increase in demand for internal multi-band antenna. It is because of this; Liu et al. produced a new dual band PIFA design in [5] (shown in Figure 2.4).

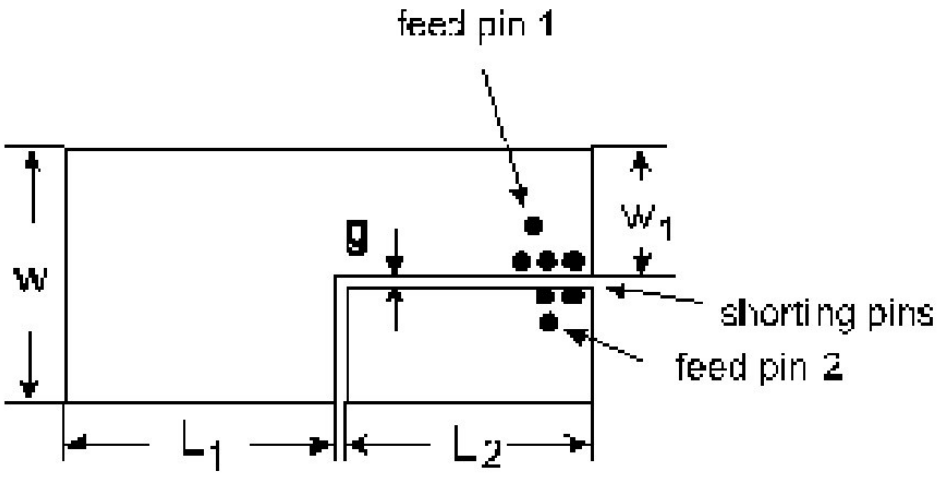

Figure 2.4: A Dual Band PIFA by Liu et al. [5]

Multi-band Planar Inverted-F Antenna has an important feature – its size is almost the same as that of a single band PIFA (having the same resonant frequency). The antenna geometry of this PIFA consists of two separate radiating elements (for 1800MHz and 900MHz), which have a radiation patterns that are omnidirectional at the resonant

frequencies. The mutual coupling between the two radiating elements is found to be good and isolation is less than –17 dB at both resonant frequencies [5]. In addition, the bandwidths of the antenna are close to those required for the two systems, 63 MHz for GSM900 and 110MHz for DCS1800. Having seen these results, PIFA is now deemed capable of multi-band operations with good performance. And that is why now the popularity of PIFA is increasing.

2.4 Other multi-band antenna design

Having seen the microstrip antenna (MSA) and Planar Inverted-F Antenna (PIFA), let us now look at two other designs, which are also used for mobile phone operations. First, is a design by Fang et al. [6], in this proposed design, a planar triple band antenna is used for operations on the GSM900 and DCS1800 networks, and GPS system. As shown in Figure 2.5, it consists of two triangular antennas that are printed on a substrate of relative permittivity $\in$r1 and thickness $h1$. The third frequency band is integrated by adding an additional microstrip patched antenna on the back of the ground plane of the triangular monopole antenna. It is printed on a substrate of relative permittivity $\in$r2 and thickness $h2$. To integrate the 3 frequency band, a feeding network consisting of the lumped-element RLC-circuits is added to obtain broadband impedance matching for the 3 frequency band. It is then observed that the impedance bandwidths, determined from 10dB return loss, are 21.7% referenced to 920MHz for GSM900 and more than 33% referenced to 1795MHz for DCS 1800. On top of that, right hand CP radiation and omni directional patterns towards the hemisphere are also obtained for the GPS band.

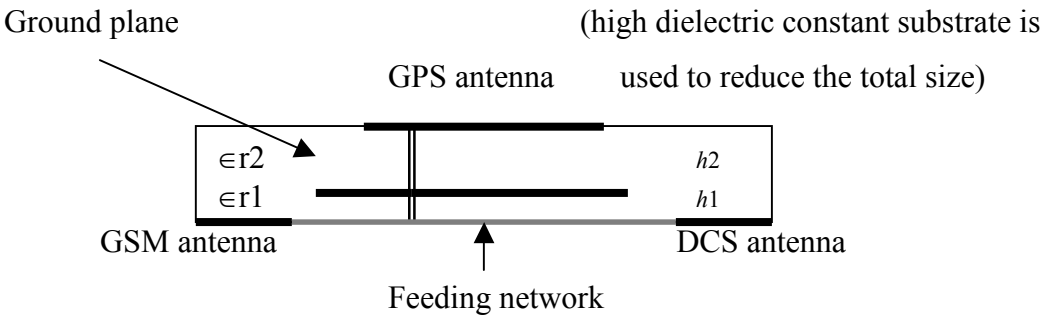

Figure 2.5: Side view of the triple band antenna

The second antenna design is a Quad Band Stubby Antenna by Borisov et al. [7]. The concept of this proposed antenna is to be used for operation on the world's major mobile communication networks, namely AMPS, GSM, DCS and PCS. The design of this antenna uses a variable pitch helical radiator combined with a monopole strip radiator. The helical radiator has three different pitch stages, which is generally used to control the resonant frequency. The assembly of the antenna consists of a helical radiator wound round a nonconductive core plug, central radiator that serves as an antenna contact and a cover. Figure 2.6 shows the core plug with a recessed pattern which soft wire is laid to form a helical radiator and the arrangement of the variable pitch helical radiator. In the paper it is also shown that the antenna has a satisfactory return loss and gain performance. Thus the antenna is deemed to be able to operate on AMPS, GSM, DCS and PCS.

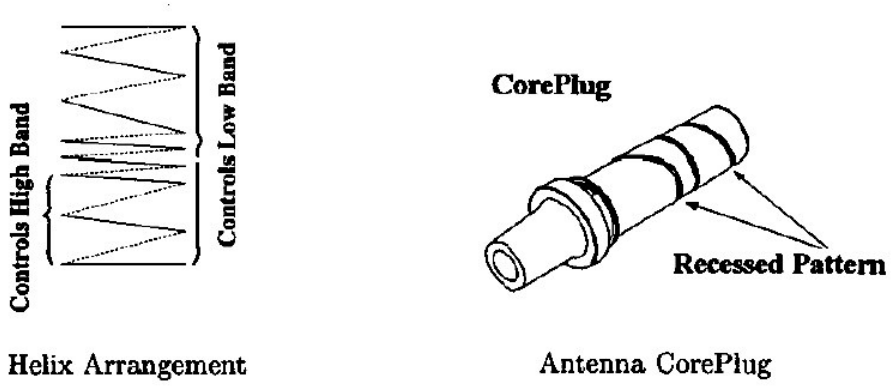

Figure 2.6: Structure of the stubby antenna

From the review of these multi-band antennas, including PIFA and MSA, it can be seen that almost all of them are able to provide satisfactory operations for wireless communications. However, among them, PIFA has more outstanding characteristics such as miniature in size and have an omnidirectional radiation pattern. Therefore in the next chapter an analysis of the PIFA will be presented.

Chapter 3

Planar Inverted-F Antenna

3.1 Introduction

Having seen the various designs of multi-band antenna, a further study will be made on the Planar Inverted-F Antenna (PIFA). Once again, this is because PIFA has proved to be the most widely used internal antenna in commercial applications of cellular communication. The main reason is that it is relatively miniature in size, which makes it suitable for an unobtrusive assembly with handheld transceivers. On top of that, PIFA has a signal characteristic of dual polarisation. This is an important requirement for all mobile transceivers as this means that the mobile transceivers can receive signals in any orientation. Another attractive feature is its multi frequencies operation, which is deemed to be an important feature for multi-band antenna designs.

This chapter presents the theory and operation of the PIFA (based on Hirasawa et al), which will be discussed using the three-dimensional electro-magnetic field time-domain analysis method called *Spatial Network Method* [2]. Although this method was not used for the designing of the antenna, its theory and operation provides a good understanding of PIFA's operations and principles.

3.2 Introduction to PIFA

The development of Planar Inverted-F Antenna (PIFA) started from an inverted-L Antenna (ILA). ILA is an antenna that consists of a short monopole as a vertical element and a horizontal wire element attached to the end of the monopole [8].

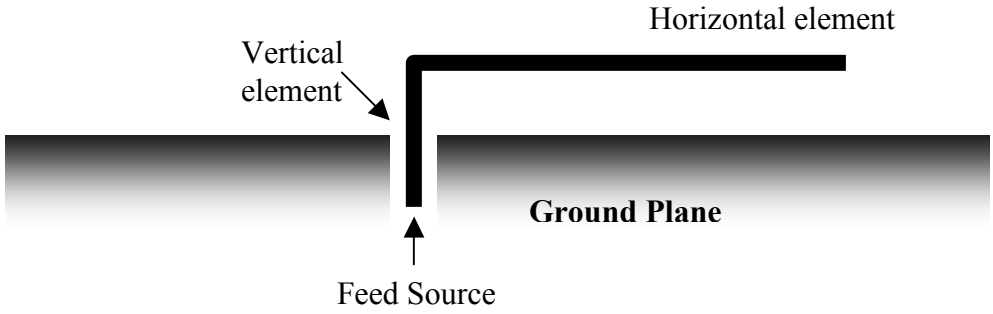

Figure 3.1: Structure of an Inverted-L Antenna (ILA) [8]

The low profile structure of an ILA is due to the vertical element's height constraint, which is a fraction of the wavelength. Due to this low profile structure, the ILA is classified as a small antenna, which in turn developed many modifications. One of these modifications is an Inverted-F Antenna (IFA), which has an additional Inverted- L element attached to the ILA. Having this modification done to the ILA, there is an increase in radiation impedance. In addition, this modification is deemed to be important because the input impedance of the IFA can be arranged to have an appropriate value to match the load impedance, without using any additional circuit between the antenna and the load [8].

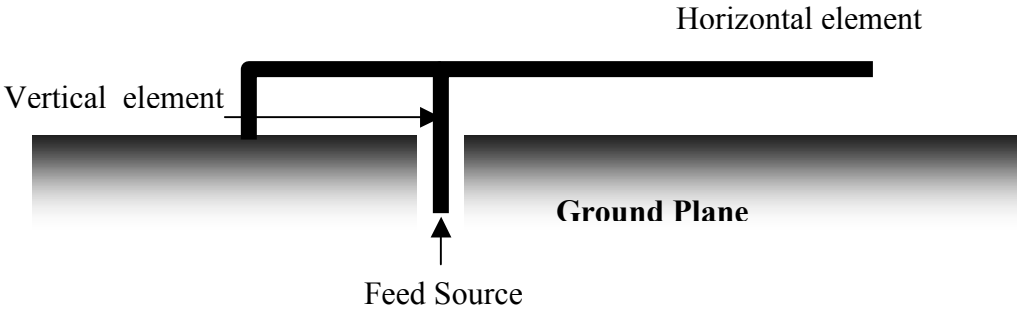

Figure 3.2: Structure of an Inverted-F Antenna (IFA) [8]

Subsequently, a further modification where the wire element in the IFA is replace by a plate is made to obtain a wider bandwidth. Thus the IFA is now called a Planar Inverted-F Antenna (PIFA).

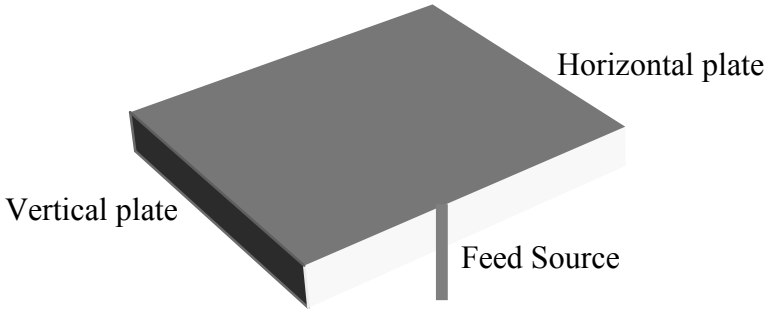

Figure 3.3: A Planar Inverted-F Antenna (PIFA) modified from IFA [8]

However, the PIFA is also sometimes referred to a short-circuit microstrip antenna (short-circuit MSA) due to the fact that the structure of the short-circuit MSA resembles that of a PIFA.

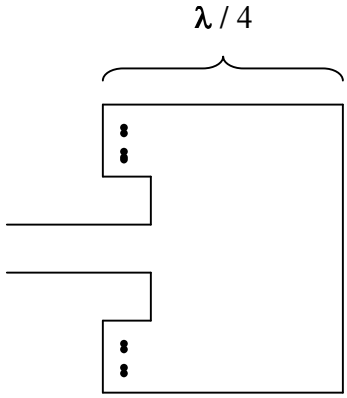

Figure 3.4: Microstrip Antenna with Shorting Pins

For these reasons, PIFA is said to have a structure between a Inverted-F Antenna and a short-circuit Microstrip Antenna [2].

3.3 PIFA Analysis by Spatial Network Method (SNM)

(Based on Hirasawa et al. [2])

In the following sections, the three-dimensional electromagnetic field time domain analysis method called the Spatial Network Method (SNM) is presented. The techniques used in this method however are of not much use in designing the multi-band PIFA. Nevertheless, some of these theories do proved to be helpful especially those concerning the width of the short circuit plate, the resonance and the PIFA bandwidth. Therefore, a brief explanation of these theories will be shown in the following sections. For a more detailed description and in depth study into this method, it is preferably to refer to the book by Hirasawa et al. [2].

3.3.1 The Analysis Model

Before a further study is made, let us look at the analysed model of the PIFA. Figure 3.5 shows the structure of the PIFA. It is fed using a 50Ω transmission line from the back of the ground plane. This transmission line consists of a centre conductor and an outer conductor, the size of which is 2Δd, where Δd is the distance between similar nodes of SNM [2]. The analysis area for the PIFA is set to 70Δd in the x direction, 75Δd in the y direction and 50Δd in the z direction. The reason for setting this analysis area is so that the input impedance is not affected.

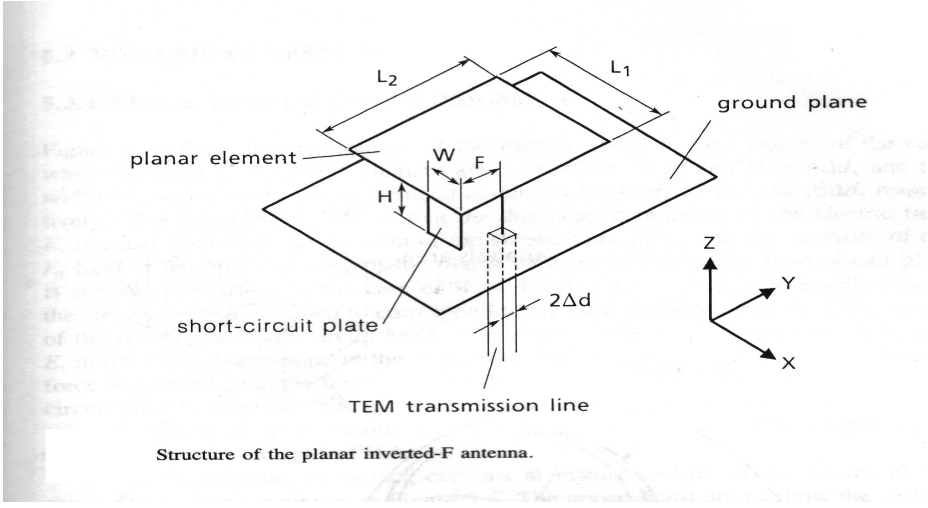

Figure 3.5: Structure of the Planar Inverted-F Antenna [2]

When a pulse wave is inserted into the TEM transmission line, the reflection wave is observed in the time domain. This reflection coefficient at the observation point can be obtained by transforming the time-domain data into frequency domain by using the Fourier transformation. Analysing the resonant frequency and the bandwidth characteristics of the antenna can then be done by determining the position of the feed source, which the minimum reflection coefficient is to be obtained. Then by inputting a sinusoidal wave with the resonant frequency into the TEM transmission line,

3.3.2 Electric Field Distribution

Having said that the electric field distribution at resonance is obtained from the amplitude of the electric node, we shall now look at the results. Figure 3.6 show the distribution of the electric field E_x, E_y and E_z in the case when the sizes of the PIFA are $L_1 = L_2 = 16\Delta d$ and $H = 4\Delta d$, and the width of the short-circuit plate varies between $2\Delta d$, $4\Delta d$, $8\Delta d$, $12\Delta d$ and $16\Delta d$.

From the results, it can be seen that the dominant component of the electric field E_z is equal to zero at the short-circuit plate while the intensity of the E_z field at the opposite edge of the planar element is significantly large. And in the E_x and E_y field, there is a pointy part which corresponds to the feed source. Based on the results it means that the electric line of force is directed from the feed source to the ground plane. Then when the width of the short-circuit plate is narrower than the planar element, the electric field E_x and E_y start generating at all open-circuit edges of the planar element. These fringing fields are the radiating sources in PIFA.

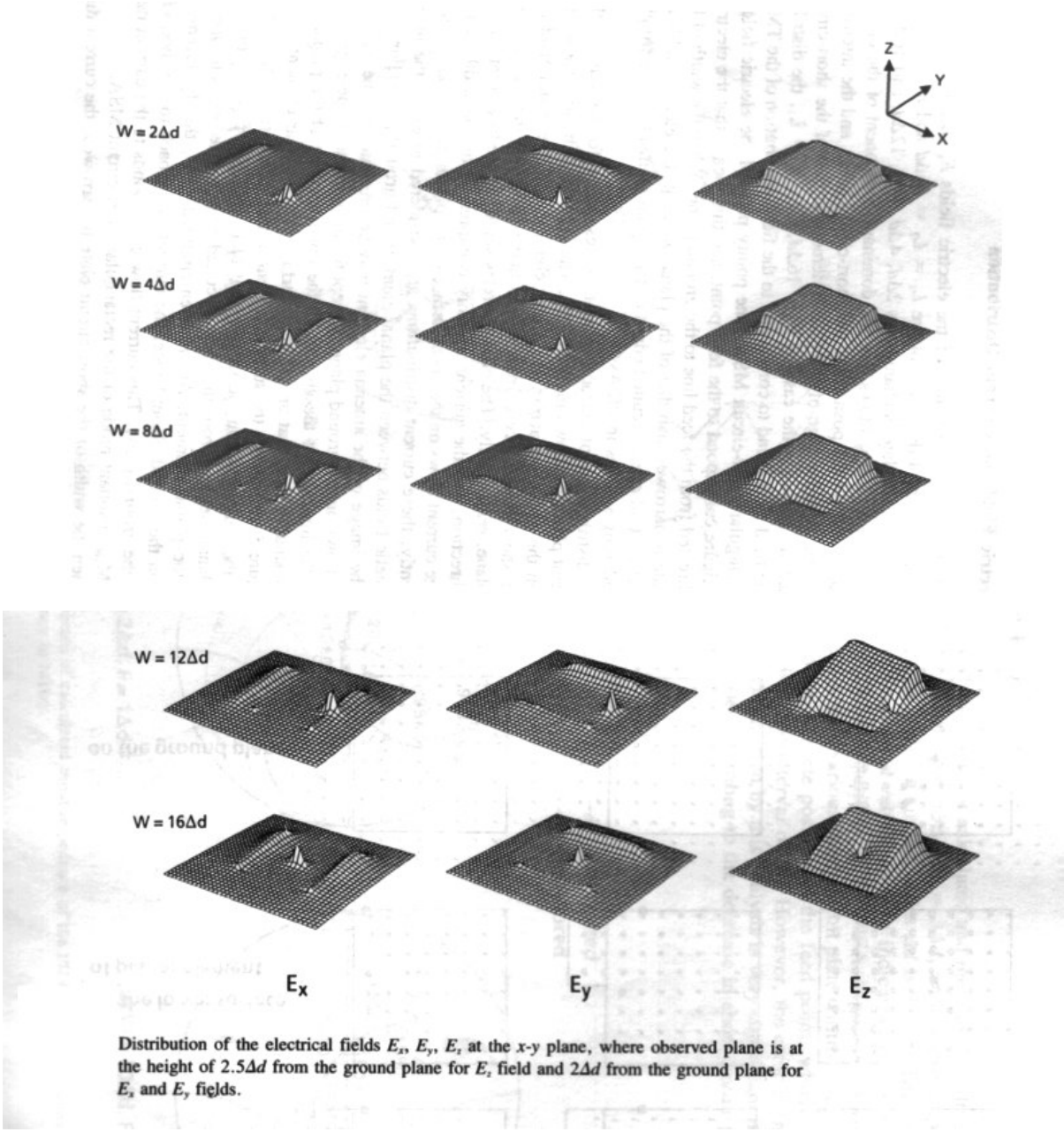

Distribution of the electrical fields E_x, E_y, E_z at the x-y plane, where observed plane is at the height of $2.5\Delta d$ from the ground plane for E_z field and $2\Delta d$ from the ground plane for E_x and E_y fields.

Figure 3.6: Distribution of electric field E_x, E_y, E_z at the x-y plane [2]

3.3.3 Current Distribution

Knowing that the current distribution at resonance can be obtained from the magnetic node component, a further study on the results was conducted. The results of surface current distributions at various widths of the short-circuit plates are shown in Figure 3.7. Based on this figure, the circles illustrate the feed source, the arrows shows the direction of the current and the current intensity is expressed by the width of the arrow. Very large current flows on the undersurface of the planar element and the ground plane compare to that on the upper surface of the element; consequently, these current distributions are considered to excite the inner electric and magnetic fields between the planar element and ground plane. From the figure it also can be seen that as the width of the short-circuit plate narrows, the current distribution varies and the effective length of the current flow on the short-circuit plate and planar element becomes longer. Therefore, the resonant frequency will be lowered and PIFAs that are smaller that the short-circuit MSAs can be operated.

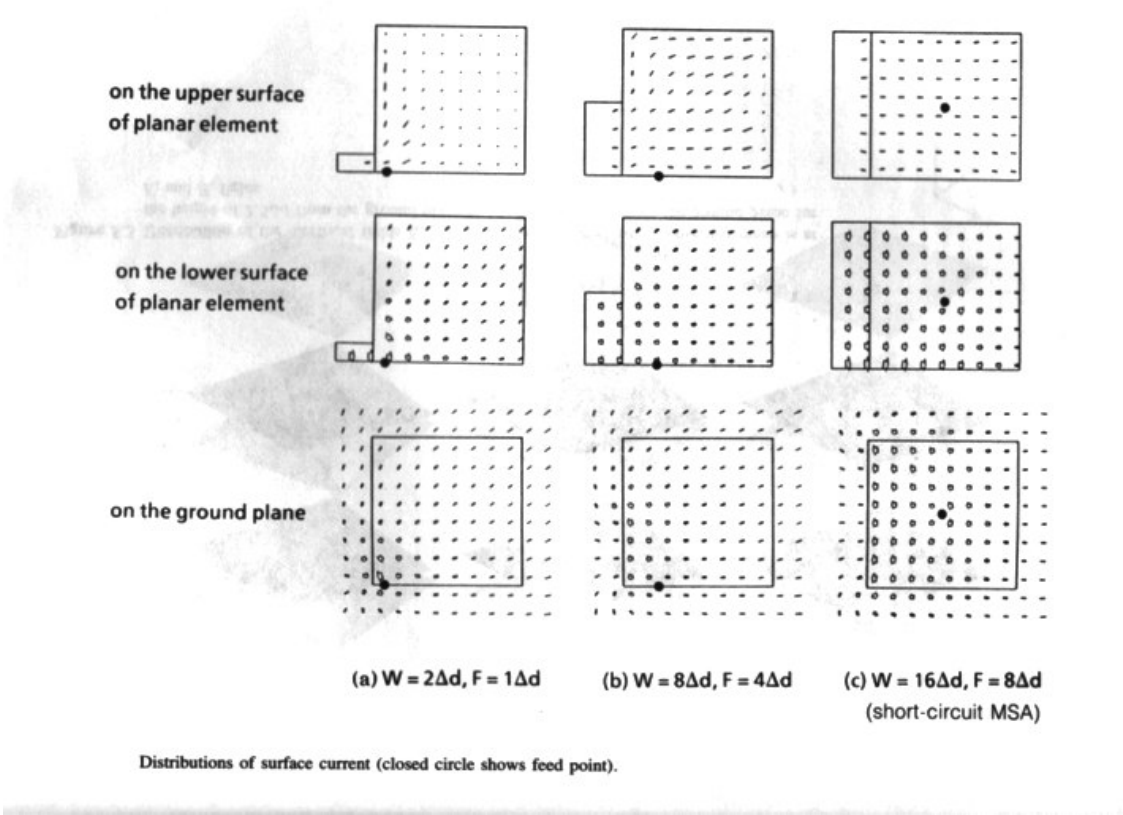

Figure 3.7: Distribution of surface current [2]

3.3.4 Resonant Frequency

The resonant frequency of the PIFA is usually determined by two major factors. One of the factors is the dimension of the short-circuit plate and the other is the dimension of the planar element. These two factors not only greatly affect the radiating frequency but also the performance of the PIFA. In addition to the two factors, there are many other reasons that contribute to the operations of this sensitive antenna. One of the factors, which cause a difference in the results, is the position of the feed source, which must be located at the electrical nodes with the interval of Δd. This difference in results according to Hirasawa et al. is approximately smaller than 3%, and it also reveals the approximation by SNM analysis is very significant in practice. In Figure 3.8, the resonant frequencies of the PIFA with various short-circuit plate width is shown. It can also be seen that the calculated results are very close to the measured values, and this indicates that the SNM is useful in analysing the frequency characteristics of the PIFA. And the main concept here is that the resonant frequency decreases with the decrease in short-circuit plate width. From the results, it can be concluded that the size of the PIFA can be smaller than the short-circuit MSA.

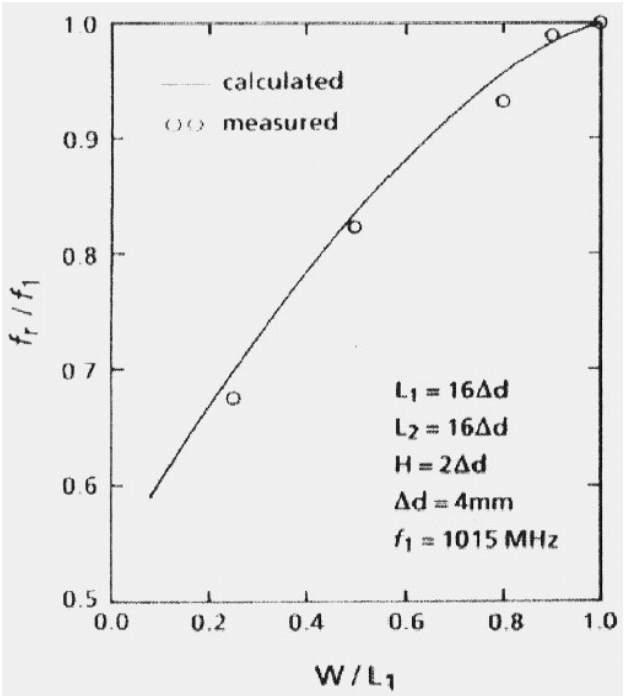

Figure 3.8: Comparison of calculated resonant frequency and experimental results [2]

Next, a study will be made on the results of the characteristics of the resonant frequency with respect to the size ratio of the planar element, L_1/L_2, shown in Figure 3.9. The change of this ratio is done only with the variation of the width, L_1.

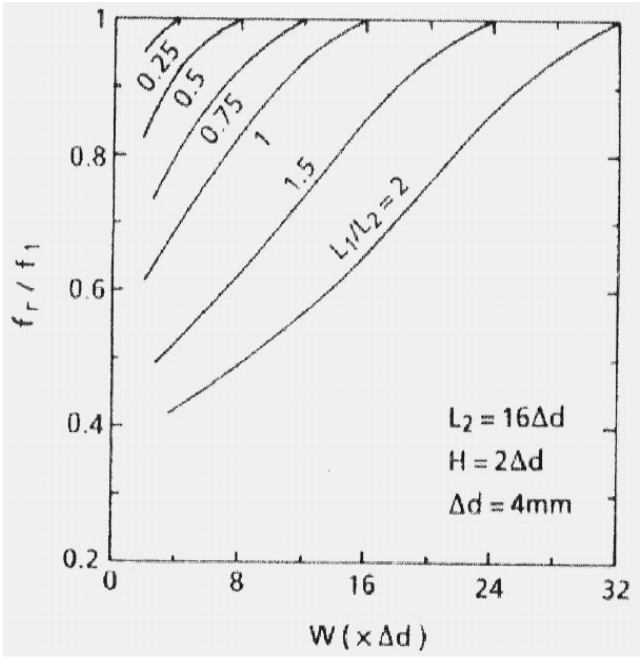

Figure 3.9: Variation of resonant frequency due to changes in size ratio of the planar element, L_1/L_2 [2]

The figure above proved that as the size ratio increases, the larger is the drop in resonant frequency with respect to the ratio, W/ L_1. Another finding from this result is that for the size ratio, $L_1/L_2 > 1$, there is an inflection in the resonant frequency characteristic when $L_1 - W = L_2$. This inflection is due to the change in current flow on the undersurface of the planar element. From Figure 3.10, it is shown that the current will flow to the open circuited edge on the long side of the planar element for $L_1 - W < L_2$. As in the case when $L_1 - W > L_2$, the current will flow to the open circuited edge on the short side of the planar element.

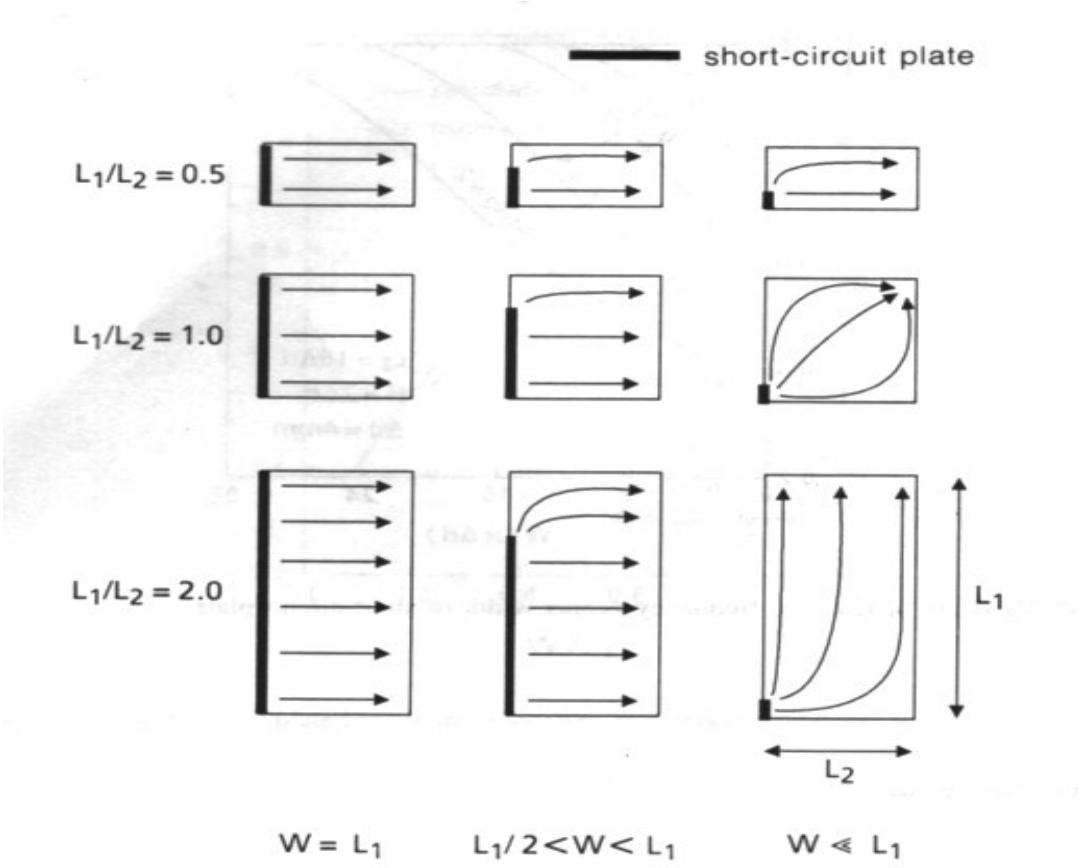

Figure 3.10: Variation of surface current flow due to the size ratio of the planar element and width of the short-circuit plate [2]

The resonance of PIFA can be expressed by

$$L_1 + L_2 = \lambda / 4 \qquad (3.1)$$

where λ is the wavelength of the resonance frequency

However, this formula does not include the variation of short-circuit plate width, W. Therefore from the analysis results of the surface current, the quarter wavelength at resonance is equal to the effective length of the current flow on the short-circuit plate and planar element.

Thus in the case when $W/L_1 = 1$, the resonance can be expressed by

$$L_1 + H = \lambda / 4 \qquad (3.2)$$

and when $W = 0$,

$$L_1 + L_2 + H = \lambda / 4 \qquad (3.3)$$

Hirasawa et al. also reported that when the antenna height is sufficiently shorter than the wavelength, the fringing effect in the open-circuited edge can be neglected, and the resonant frequency calculated by (3.2) and (3.3) agrees with the measured results, with an error of 3%. And also the resonant frequency, f_r, in the case of $0 < W / L1 < 1$, can be expressed by:

$$f_r = r * f_1 + (1 - r) * f_2 \qquad \text{for} \qquad L_1 / L_2 \leq 1 \qquad (3.4)$$

$$f_r = r^k * f_1 + (1 - r^k) * f_2 \qquad \text{for} \qquad L_1 / L_2 \geq 1 \qquad (3.5)$$

where $r = W/ L_1$, $k = L_1 / L_2$, and resonant frequency f_1 is expressed by (3.2)

For the resonant frequency, f_2, it is expressed by:

$$L_1 + L_2 + H + W = \lambda / 4 \qquad (3.3)$$

3.3.5 Bandwidth

The bandwidth of a PIFA is usually affected by the ratio of L_1 / L_2 and the dimension of the short-circuit plate's width, W. This can be clearly seen from the results obtained from the analysis by Hirasawa et al., which is shown in Figure 3.11 and 3.12. A comparison of a conventional MSA was made with a variation of W and the ratio L_1 / L_2 on the PIFA. This is to observe the effect they have on the bandwidth.

In Figure 3.11, the characteristics of the relative bandwidth for VSWR of 1.5 are shown when the width of the short-circuit plate W is equal to the width of the radiating planar element L_1, which corresponds to that of a short-circuit MSA.

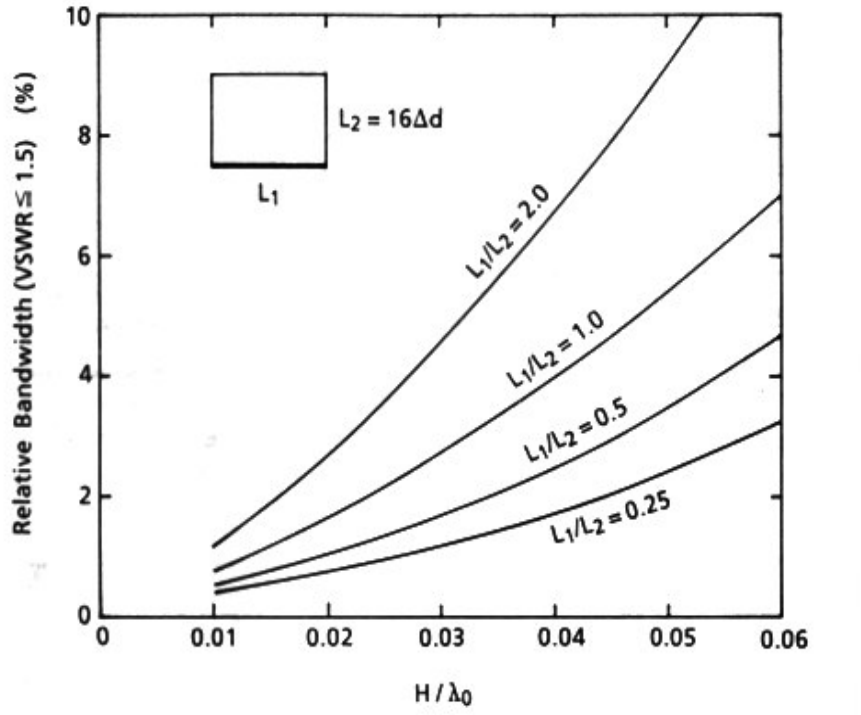

Figure 3.11: Bandwidth of the PIFA when the width of the short-circuit plate W is equal to the width of the radiating planar element L_1 [2]

In the following graph (Figure 3.12), the width of the short-circuit plate W is made to be less than the width of the radiating planar element, $W < L_1$, with the same VSWR from the previous graph. The broken line shows the bandwidth of a short-circuit MSA or a PIFA with $W/ L_1 = 1$.

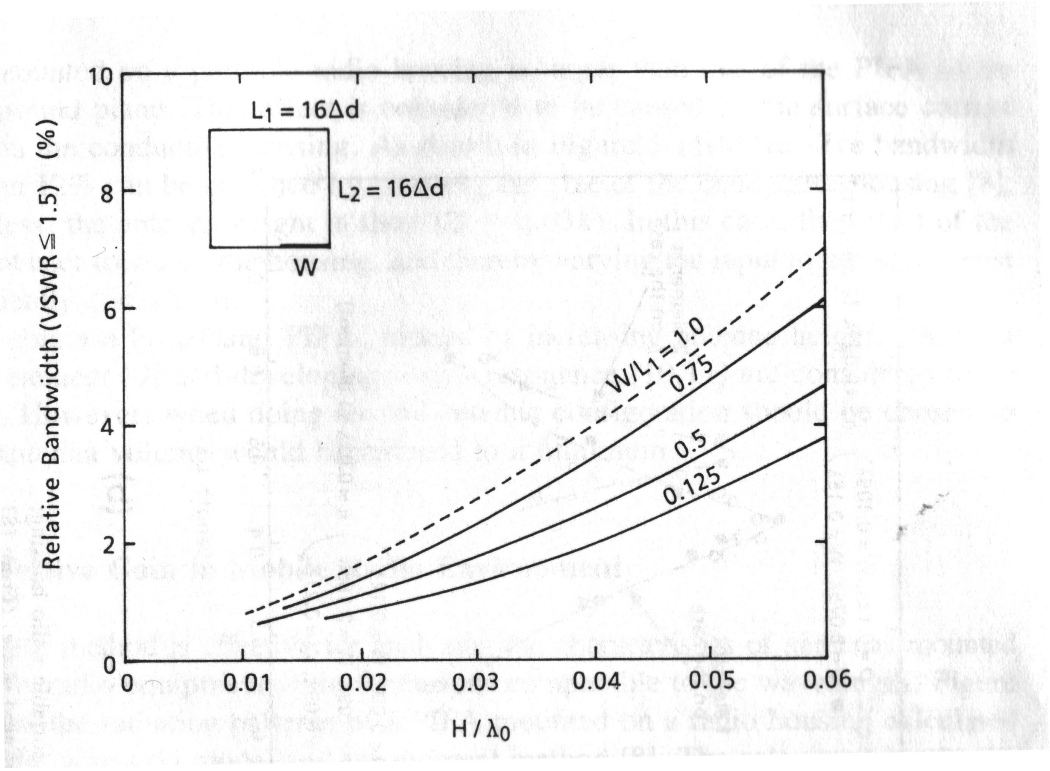

Figure 3.12: Bandwidth of the PIFA when W < L_1 [2]

Conclusion is derived form these two graphs that a decrease in the width of the short-circuit plate of the PIFA means a reduction in bandwidth. It can also be seen from the graphs that a rise in height H can lead to an increase in the bandwidth.

3.4 Dual Polarisation

Dual polarisation means that an antenna can transmit and receive both horizontally and vertically polarised waves. This is an excellent characteristic that made PIFA such a good antenna for use in a handheld transceiver. Furthermore, PIFA has a dual polarisation capability of radiating two orthogonal field components with nearly the same magnitude, where a microstrip antenna has only one field component that dominates in magnitude. This unique property lies in the fact that all four edges of the PIFA radiates almost equally, while in MSA radiation occurs only from its two opposing edges with one dominant linearly polarised field [9]. For that reason, PIFA is deemed to be a good antenna for use with mobile communications, because regardless

how the handheld transceiver is orientated, it is able to receive signals. And so for this thesis, PIFA was chosen to be the basic design as the final antenna design will be for use in a handheld transceiver.

Chapter 4

Methodology

4.1 Introduction

The design of the multi-band Planar Inverted-F Antenna (PIFA) is very complex and tedious. It can be seen in the later part of this thesis that even a difference of 0.5mm in the antenna can shift the resonant frequency by 50MHz or halve the return losses. This is due to the characteristics of the PIFA, which are very sensitive to dimension changes and the effects of the ground plane. Although much of its operations and characteristics are already known, it is does not mean that everything is understood in the designing of the PIFA. In fact, many current methods of PIFA designing in practical applications are still being done through a trial and error process. Therefore, a lot of time and patience is required in designing the multi-band PIFA.

Having been introduced to the background, theory, design and development of the Planar Inverted-F Antennas, we will now look at the results for the antennas that have undergone a great deal of simulations. In this chapter, the simulation results will be discussed and compared with the ideal solutions or theoretical results. Also included in this chapter are the effects of dimension changes, the ground plane and the shifting of feed source on the PIFA. On top of that, the steps in developing simple single band Planar Inverted-F Antennas operating at 900MHz, 1.8GHz, 2.0GHz and 2.4 GHz respectively will be discussed. Next, the design of a triple band E-shaped PIFA based on W. Dou's et al. design will be analysed. Finally the development process of the newly designed quad band PIFA will be shown.

4.2 Selection Criteria

The criteria of this thesis is to design an efficient, small and low profile antenna with multi-band operations for use on a handheld transceiver. In addition, this antenna must include the operation for use on GSM900, GSM1800 and UMTS networks. Thus, to start with, a range of miniaturised multi-band handheld transceiver antenna was being studied (some of which are presented in Chapter 2). The research uncovered several possibilities including Microstrip Antenna, Planar Inverted-F Antenna (PIFA) and other multi-band antenna designs. Among these antennas, PIFA is the most promising candidate due to its various advantages mentioned in previous chapters. Therefore, extensive studies were made on PIFA to learn about the various designs and methods employ to develop a multi-band PIFA.

At present, there are many methods of designing multi-band PIFA. One of those methods has been achieved by using EM coupling between several separate elements; usually one element is fed by a coaxial line and the others are parasites [10]. Although this method is effective for multi-band antenna design, but a large space is required for the installation of the antenna. Another design method using separate elements, which also allows multi-band operation, has a feature of having the size of that of a single band PIFA (seen in the design by Liu et al.). Other method including a design by Salonen et al. [11], which achieved dual band operation by cutting a U-shaped slot in the patch, and a tri-band PIFA by Dou et al. [12] were also being studied.

However, after learning about these multi-band PIFA's characteristics and investigating their performance (using simulation software), it was found that some of the methods used could not produce satisfactory results (probably due to the lack of understanding of these methods). Nevertheless, in spite of the failures, the search for a method to design a new multi-band antenna continues.

Subsequently, after numerous attempts of simulation, it was found that the control on the design of Dou's et al. PIFA was considered to be the easiest among those mentioned earlier. In addition, it has very good feature such as having the same size of that of a

single band PIFA. The reason for that is because it does not use separate elements to achieve multiple frequency bands operation. Instead, multiple frequency bands operation of the PIFA is achieved by simply having two narrow linear slots etched on the same side of the antenna. However, the strongest influence was perhaps the antenna is able to operate at a frequency ratio of 1.04, which was confirmed by the results from the simulation runs. Due to the close frequency band operation of the GSM1800 and UMTS, which requires a frequency ratio of 1.11, the antenna was deemed to be a favourable advantage for implementation of the criteria. Thus knowing the outstanding advantages of this antenna, the preliminary design was based on it.

Then another decision was made on the design of the antenna was to include a non-cellular frequency band operation. Based on the current situation, it was found that having an additional function of the new Bluetooth wireless system to be included onto the mobile phone is desirable. The reason is because Bluetooth wireless system, which is used to provide links between computers and peripherals, Persona Digital Assistants (PDAs) and mobile phones, can be very useful for users to transfer of data and to access the Internet via the mobile phones. Moreover this implementation could see the new antenna design being used for other handheld transceivers such as PDAs. Thus Bluetooth operation was included as a non-cellular frequency on to the antenna.

Finally with the basic design of the antenna fixed, trials on simulation will be performed to check the viability to incorporate an additional frequency band to the antenna. And if time permit, the final design of the quad band antenna would be constructed to verify the results obtain from the simulations.

4.3 Simulation Software *FEKO*

Taken significantly from FEKO's user manual.

Before designing the PIFA, we will look at the functions of the simulation software, FEKO. It is simulation software used for electromagnetic analysis to obtain parameters such as return losses and radiation pattern. The name FEKO is an abbreviation derived from the German phrase **Fe***ldberechnung bei* **K***örpern mit beliebiger* **O***berfläche.* (*Field computations involving bodies of arbitrary shape.*) As the name suggests, FEKO can be used for various types of electromagnetic field analysis involving objects of arbitrary shapes.

The program, FEKO, is based on the Method of Moments (MoM) techniques. Electromagnetic fields are obtained by first calculating the electric surface currents on conducting surfaces and equivalent electric and magnetic surface currents on the surface of a dielectric solid. The currents are calculated using a linear combination of basis functions, where the coefficients are obtained by solving a system of linear equations. Once the current distribution is known, further parameters can be obtained e.g. the near field, the far field, radar cross sections, directivity or the input impedance of antennas.

Electrically large problems are usually solved with either the Physical Optics (PO) approximation and its extensions or the Uniform Theory of Diffraction (UTD). In FEKO these formulations are hybridised with the MoM at the level of the interaction matrix. This is a major step in addressing the problem of solving electromagnetic problems where the object under consideration is too large (in terms of wavelengths) to solve with the MoM but too small to apply only the asymptotic UTD approximation with high accuracy. With the hybrid MoM/PO or hybrid MoM/UTD techniques, critical regions of the structure can be considered using the MoM and the remaining regions (usually larger, flat or curved metallic surfaces) using the PO approximation or UTD.

FEKO has three many user interface, namely WinFEKO, EditFEKO and GraphFEKO. EditFEKO is a customised text editor for the input of solution and the main control to

generate simulation results for use in WinFEKO and GraphFEKO. WinFEKO is a user interface module used to view the solution of a problem. It is able to perform 3D visualisation, which includes surface currents, near field contour plots and 3D radiation pattern plots. And finally, GraphFEKO is used to generate polar plots, linear plots and graphs. With the capabilities of FEKO, a lot simulation can perform to obtain output parameters such as specific absorption rate (SAR), return losses and radiation patterns.

4.4 Simple Single Band PIFA

Before beginning with the development of the quad band PIFA, we will look at the designing process of a simple single band PIFA and the characteristics of each single band PIFA at the different propose frequency bands. This designing had helped the author to understand the characteristics and various factors that determine the performance of the PIFA. Using the design parameters given in Chapter 3, the basic dimensions of the PIFA is being derived using the following equation.

$$L_1 + L_2 \approx c / 4f_r \qquad (4.1)$$

where f_r is the resonant frequency.

The resulted dimensions for the PIFA based on equation (4.1) are:

900MHz PIFA:

$L_1 = 27mm$

$L_2 = 56mm$

1800MHz PIFA:

L1 = 14mm

L2 = 28mm

2GHz PIFA:

L1 = 12.5mm

L2 = 25mm

2.4GHz PIFA:

$$L1 = 10.5mm$$

$$L2 = 21mm$$

Having derived the basic dimensions, a trial and error process commence to develop new dimensions for the PIFA to perform to its requirements. And with the use of FEKO, several attempts were made to obtain the desired resonant frequency and bandwidth by changing L_1, L_2, W, H, feed source's position and the ground plane's dimension.

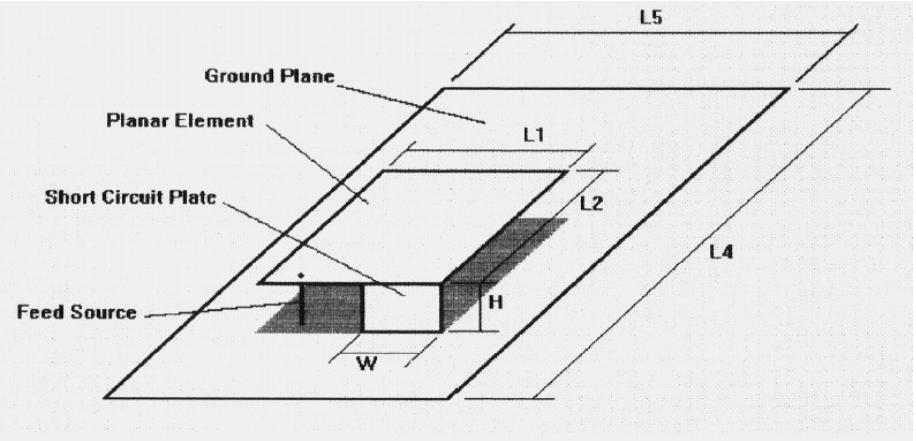

Figure 4.1: Structure of a Single Band PIFA

First of all, with the basic dimension for the 900MHz PIFA, additional dimensions such the height (H), the width of the short-circuit plate (W) and the position of the feed source was estimated based on knowledge from the researches. However the ground plane was made be infinite due to the lack of knowledge and advice. With all these necessary data, simulation was performed using FEKO.

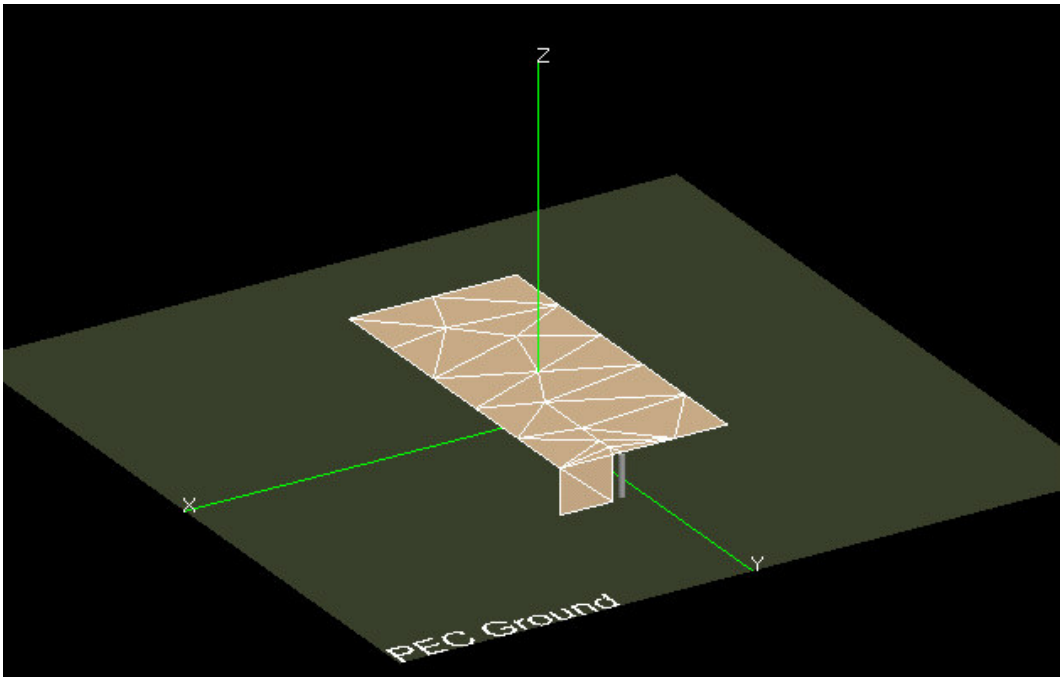

Figure 4.2: 900MHz PIFA with an Infinite Ground displayed in FEKO

The results obtained were very encouraging, with a return loss of approximately –21.7dB at 1028MHz. With this success, it prompted that work should proceed to investigate the effects of a finite ground. Thus research was again carried out to find a solution for defining a finite ground plane. Nonetheless, without much hassle a discovery was made from a thesis done by a student in University of Queensland [9]. Facing the similar problem as that student did, the solution presented in that thesis became an instant answer. Therefore, without changing the dimension of the patch, a similar finite ground plane (shown in Figure 4.3) is being defined.

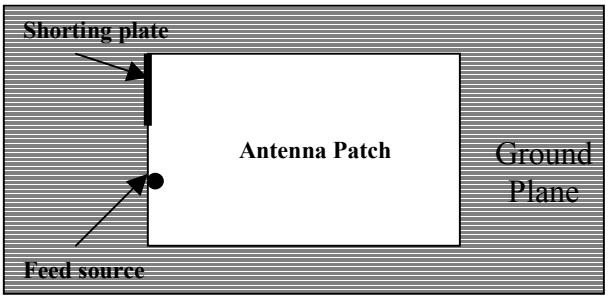

Figure 4.3: 900MHz PIFA with a Finite Ground Plane

However, the results obtained after adding a finite ground plane was considered a total failure with a return loss of –0.29dB at 2135MHz. Alterations to the antenna patch did not help to improve the situation, instead it got worse. Although further research was being done to find an answer to the problem, it was not fruitful. Thus a trial and error process was carried out to change the ground plane's dimension and the antenna patch's parameters. Finally after numerous simulation runs, it was found that the position of the antenna patch could prove to be a problem. So, the design process in back on track again and a new design with successful results is shown in Figure 4.4.

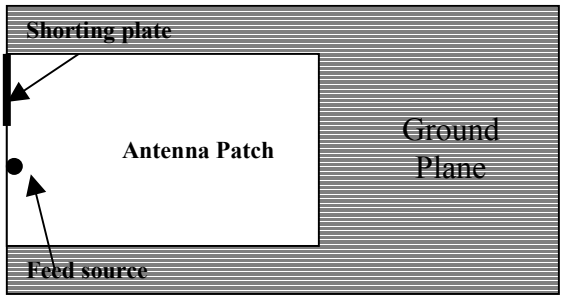

Figure 4.4:Successful implementation of Finite Ground Plane with 900MHz PIFA

After numerous attempts, it came to light that when the antenna patch is shorted to the edge of the ground plane there was a remarkable improvement. With a return loss of –22dB at 1000MHz, the antenna proved to be able to work on a finite ground plane similar to that simulate on an infinite ground plane. Hence without much hesitation, the various dimensions of the antenna patch were varied to achieve an optimum return loss at the desired frequency. And with the knowledge gain from the researches, the resonance of the antenna depends on size of the antenna patch; patch size was changed to conform to the desired frequency. As a result, the optimum dimension of the antenna patch was achieved with a return loss of –24dB at 900MHz. However, the effects of the other parameters of the antenna had not been examined, so another process of trial and error was performed on the various parameters of the antenna. First it was found that the width of the short-circuit plate could affect the resonant frequency, which agreed to the theory that is presented by Hirasawa et al. (Chapter 3), i.e. resonant frequency decreases with the decrease in short-circuit plate width, shown in Figure 4.5.

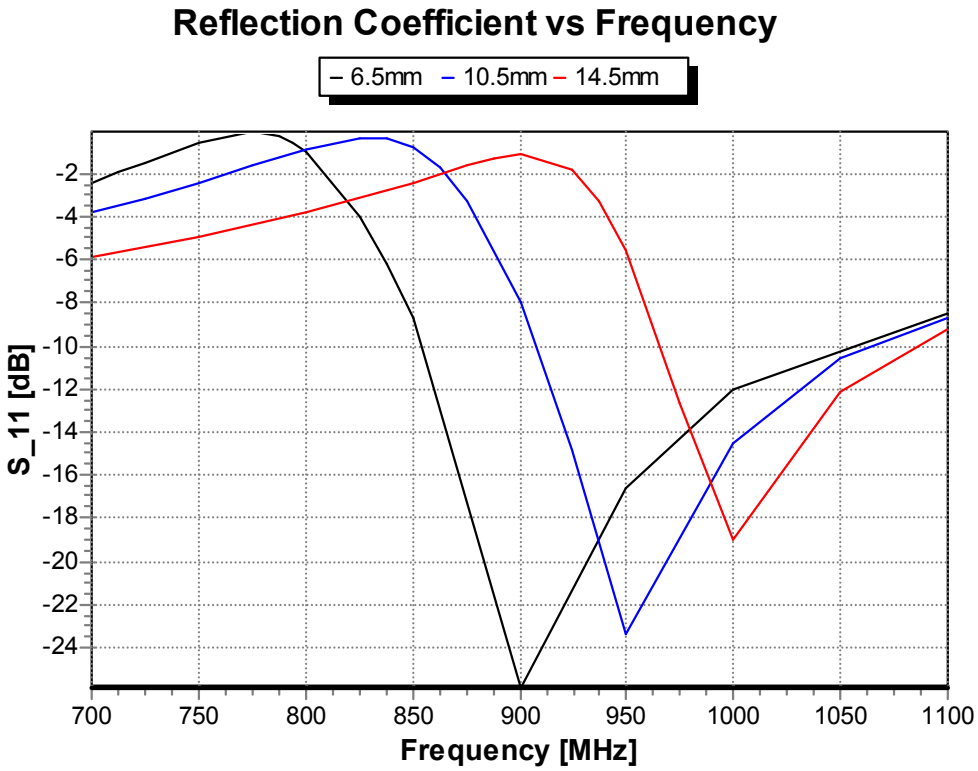

Figure 4.5: Simulated Return Loss for 900MHz PIFA with varying Short-circuit Plate Width, W

Next the effects of changing the height of the antenna patch from the ground, H, were being investigated (results are shown in Figure 4.6). It was found to be that resonant frequency decreases with the increase in height of the antenna patch.

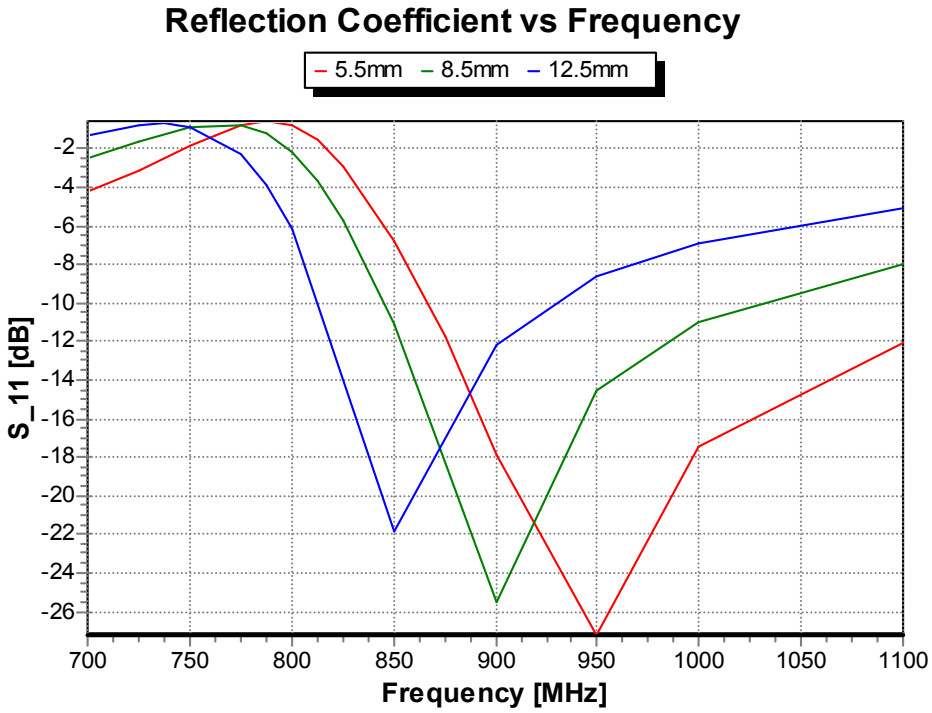

Figure 4.6: Simulated Return Loss for 900MHz PIFA with varying Height of the Antenna Patch, H

So looking at an equation from chapter 3,

Equation (3.3): $L_1 + L_2 + H = \lambda / 4$

With L_1 & L_2 fixed, H will increase with an increase of wavelength. Thus if wavelength increase, the frequency will decrease. With that, it was ascertained that the findings were correct.

Following that, the effects of varying position of the feed source were being analysed.

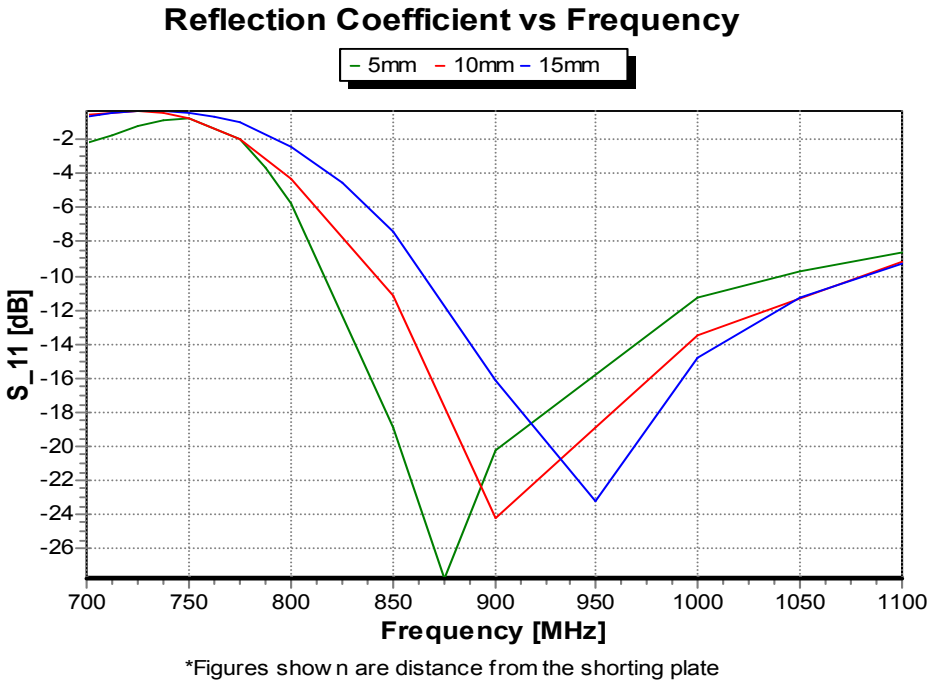

Figure 4.7: Simulated Return Loss for 900MHz PIFA with varying Position of the Feed source

From Figure 4.7, it was deduced that as the feed source get nearer to the short-circuit plate, the resonant frequency decreases.

Finally after all aspect of the 900MHz PIFA were examined, the final dimensions were determined to be:

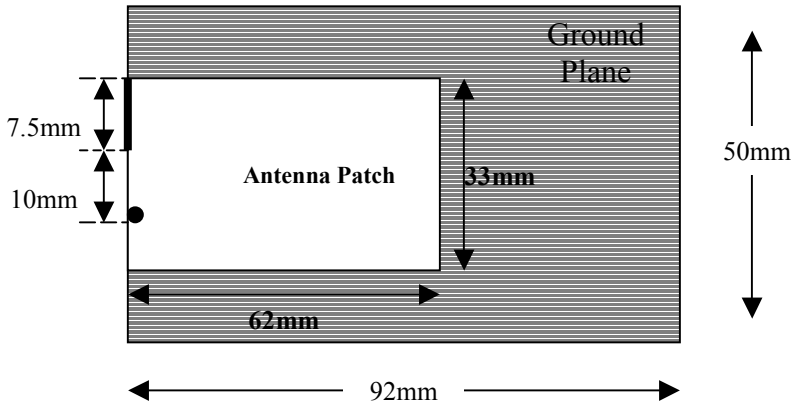

* Height of the antenna patch form the ground plane is 7.5mm

Figure 4.8: Final dimensions of the 900MHz PIFA

Subsequently, the dimensions of the PIFA for other resonant frequencies were being determined the same way as it was in the 900MHz PIFA. However do note that the feed source is shorted to the ground. Following are the dimensions,

For 1800MHz:

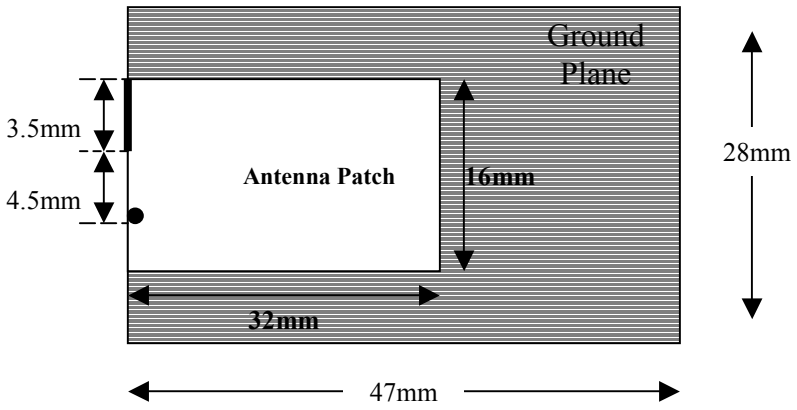

* Height of the antenna patch form the ground plane is 5.5mm

Figure 4.9: Final dimensions of the 1800MHz PIFA

For 2GHz:

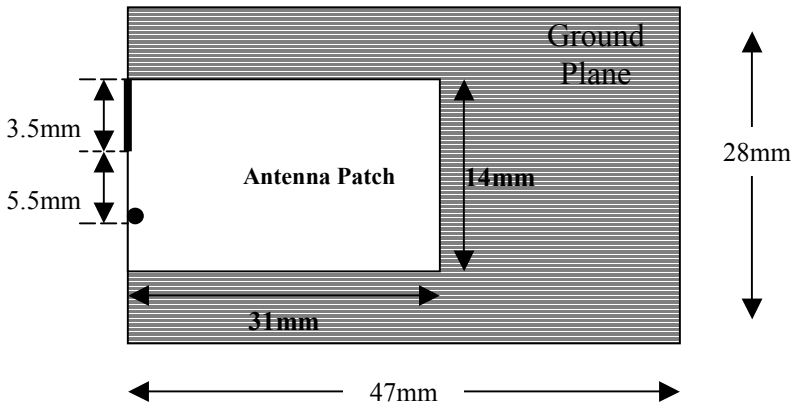

* Height of the antenna patch form the ground plane is 5.5mm

Figure 4.10: Final dimensions of the 900MHz PIFA

For 2.4GHz:

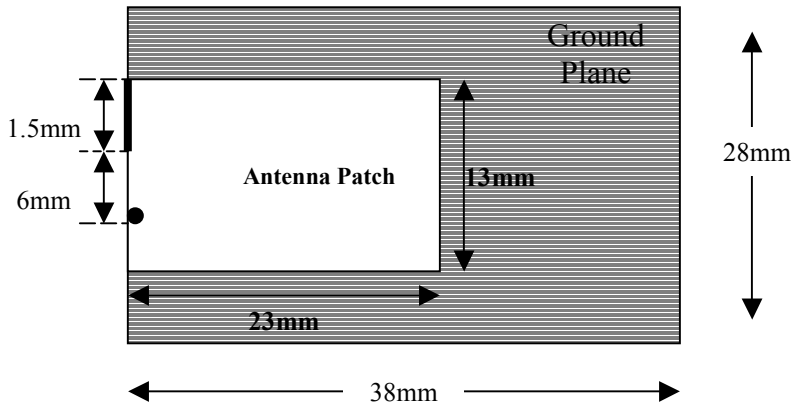

* Height of the antenna patch form the ground plane is 5.5mm

Figure 4.11: Final dimensions of the 900MHz PIFA

Finally having understood the characteristics of the PIFA work can now proceed to design the quad band PIFA. Although all experiments performed on the single band PIFA were the basics, it did proved to be very helpful in the following design process of the quad band PIFA.

4.5 Tri-Band PIFA

Since the preliminary design of the quad band PIFA is based on Dou's et al. tri-band PIFA, simulations were being performed to study the characteristic of the antenna before any work can begin on the quad band PIFA. Figure 4.2 shows the design of Dou's et al. tri-band PIFA that was entered for simulations in the FEKO.

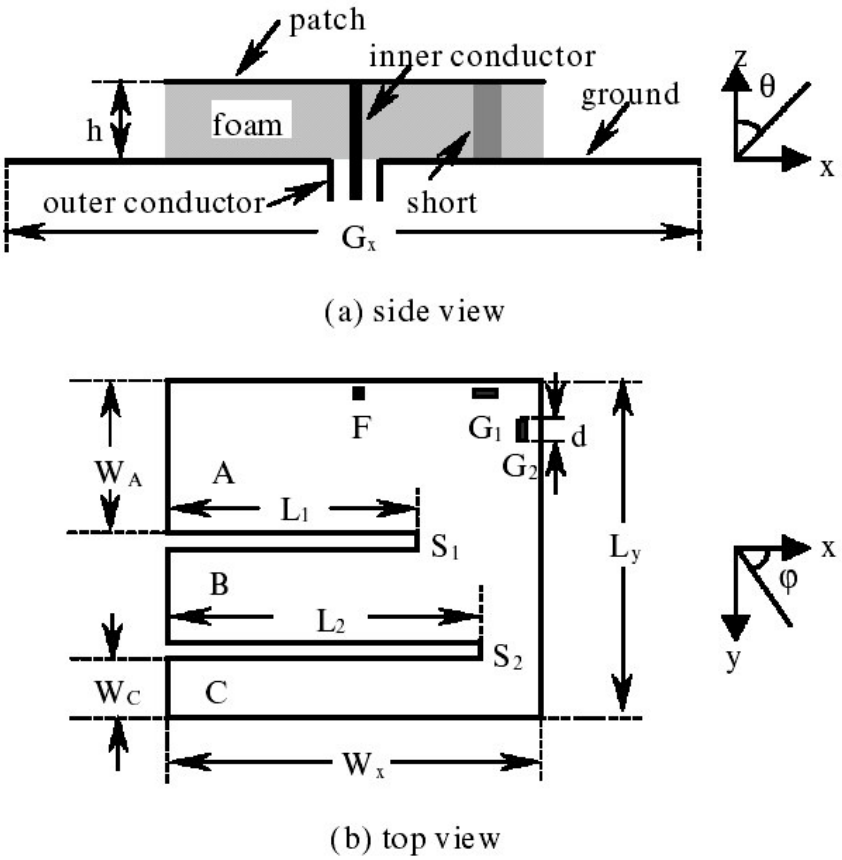

Figure 4.12: Design of Dou's et al. tri-band PIFA

After the first simulation run with the dimensions given in the paper by Dou et al., the results obtained were found to be a failure as the return loss was only about –2.6 dB. Then few alterations to the antenna patch were made to improve the situation. However, that did not help and the return losses continue to stay above –3dB. Subsequently with the knowledge gained from the single band antenna, it was noted that the position of the

antenna patch on the ground plane could be the problem, same as what happen in the single band PIFA. Thus a new placement of the antenna patch on the ground plane was entered for simulation, and the result obtained following that was good. However, this result did not perform as what was shown in the paper. Thus more trial and error processes being to search for an optimum result.

After numerous runs of simulation, the optimum result with all parameters maximised was obtained. With reference to the antenna design illustrated in Figure 4.9, the geometry for the tri-band PIFA was establish. The antenna patch is determined to be L_y x W_x = 52mm x 45mm so as to have a lowest resonant frequency of 920MHz. Foam that has the same size as the patch is also mounted on the ground plane as what is shown in the paper. Two linear slots S1 and S2 are also etched on the same side of the patch but at a different position, thus giving a new dimensions for the widths with W_A = 23.5mm, W_B = 9.8mm, and W_C = 7.7mm. In addition, the slot lengths are also changed to a suitable length where L_1 = mm and L_2 = mm. Investigations are also conducted on the antenna's characteristics that are presented in the paper. It is found that the simulation results agree to the results given in the paper. In the next chapter, the optimised results will be shown along with some discussion.

4.6 Quad Band PIFA

Although with the aid of Dou's et al. design, the designing process for the new quad band PIFA was not simple, a lot of time and effort have been spent in researches and experiments to obtain a quad band operation on the antenna. Having read and studied the operation of several multi-band PIFA designs from different sources, it was found that multi-band designs by Dou et al. and Salonen et al. are similar. In both cases, multi-band frequency operations were achieved thru etching slots onto the PIFA, with each additional slot producing an extra frequency band operation.

With the tri-band PIFA design from the previous section, a series of experiments such as etching a slot on the different sides of the antenna patch and etching a U-shape slot in the antenna patch. Finally by comparing all the results obtained, it was found that the control over the frequencies is better and easier, and better return losses can be achieved by etching all slots on the same side of the patch as compared to the other methods.

Figure 4.13 shows the structure and design of the quad band PIFA. The design of this quad band PIFA is done thru etching an additional linear slot in the patch. Dimensions from Dou's et al. design are also changed to suit the function of the new design and additionally the truncated foam is being removed.

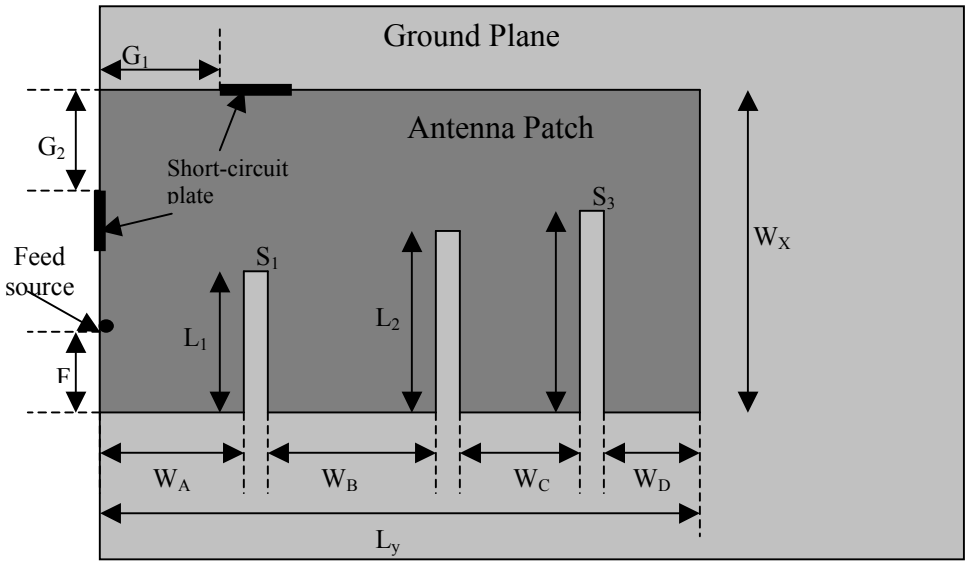

Figure 4.13: Design of the Quad Band PIFA

Nevertheless work did not stop there, instead more trial and error experiments were carried out to optimise the design to perform at the desired resonant frequencies. Then after numerous trials, a result with resonant frequencies close to that of the desired ones was achieved. However, the bandwidths did not meet the requirements, i.e. a frequency range of 880 – 960MHz is required for GSM900 operation, 1710 – 1880MHz for GSM1800, 1990 – 2170MHz for UMTS, and 2.4 – 2.5GHz for Bluetooth. Therefore, the antenna design is back to the trial and error process again. However, things did not turn out as well as it used to be, as no satisfactory results were obtained from the countless trials, instead the results usually got worse. Evidently, either the antenna structure was not working or something had been overlooked. Thus more research was conducted to find ways in increasing bandwidth. Then it was realised that the results from the single band simulations did actually show significant increase in the bandwidths. Subsequently, the varying of those dimensions such as width of the short-circuit plate, height, and the feed source position, was performed on the antenna. Eventually, a set of satisfactory results was achieved and the dimensions are as follow:

$L_y = 51.5$	$W_x = 60.0$
$L_1 = 23.6$	$W_A = 23.9$
$L_2 = 29.9$	$W_B = 3.4$
$L_3 = 33.35$	$W_C = 7.2$
$G_1 = 6.0$	$W_D = 13.0$
$G_2 = 7.0$	
$F = 22.0$	

Height = 4.0
Width of the short-circuit plate = 5.5

Having a structural orientation as shown in Figure 4.13. However, note that the feed source is shorted to the ground.

Now we shall look at how the resonant frequencies are being achieved thru the main determining factors. First of all investigation will be made on function of the three linear slots on the antenna patch. Figure 4.14, 4.15 and 4.16 show the return losses of the antenna with variation of L_1, L_2, and L_3 respectively.

Variation of slot length, L_1

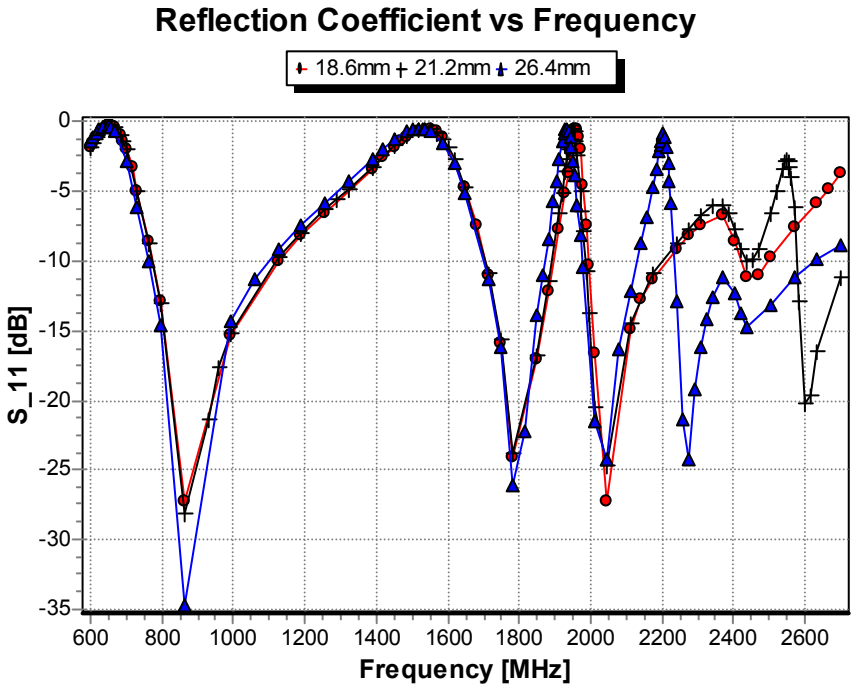

Figure 4.14: Return Loss Diagram for varying of slot S_1's length L_1

Figure 4.14 shows the return loss curve where the slot S_1 is fixed 2mm. It is expected that the first resonance will always stay at 870MHz, which confirms that this resonance is determine by the antenna patch size. It can also be seen from the graph that the second and third resonance do not shift when only L_1 is varied. However, the varying of L_1 does affect the fourth resonance. Thus it can be concluded the length of slot S_1 can be use to determine the fourth resonance.

Variation of slot length, L_2

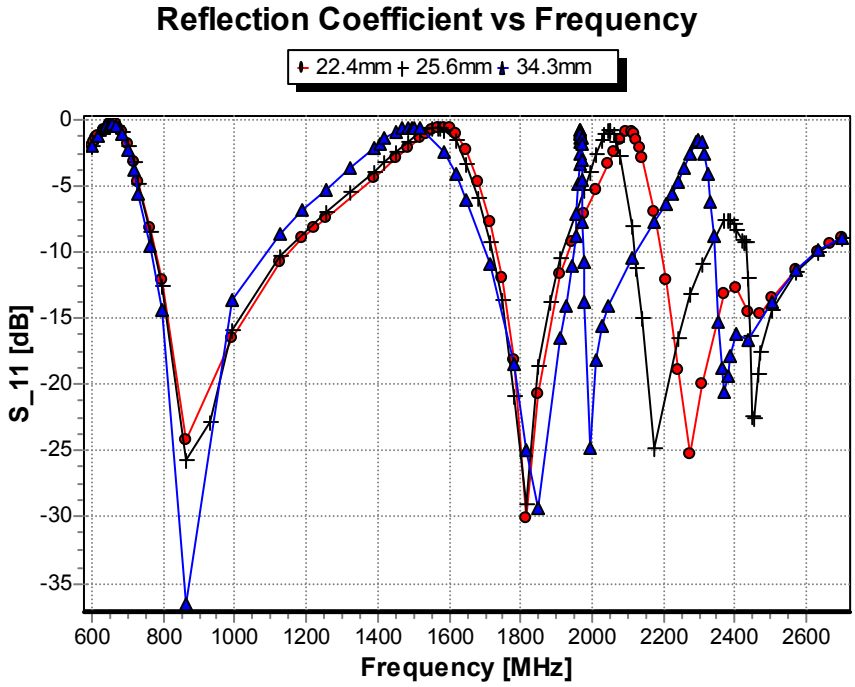

Figure 4.15: Return Loss Diagram for varying of slots length L_2

Figure 4.15 shows the return loss curve where the slot S_2 is fixed at 2mm. Similarly, it is expected that the first resonance would always stay at 870MHz. However from the graph, it can be seen that this time the second and fourth resonance do not shift when only L_2 is varied. Instead, the varying of L_2 will mainly affect the third resonance. Thus it can be concluded the length of slot S_2 can be use to determine the third resonance.

Variation of slot length, L_3

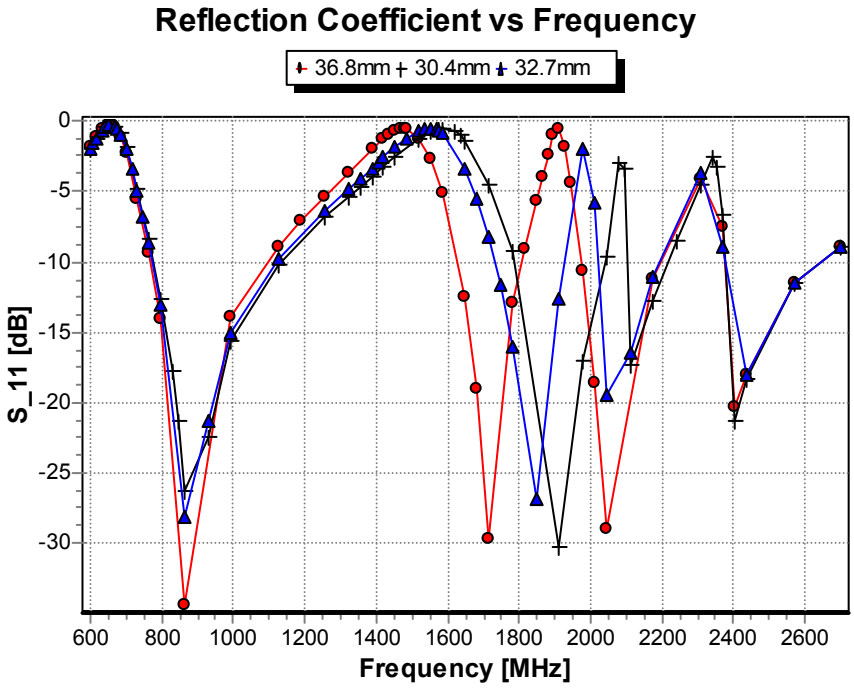

Figure 4.16: Return Loss Diagram for varying of slots length L_3

Figure 4.16 shows the return loss curve where the slot S_3 is fixed at 2mm. Similarly, it is expected that the first resonance would always stay at 870MHz. However from the graph, it can be seen that this time only the fourth resonance do not shift when L_3 is varied. Instead, the varying of L_3 will mainly affect the second resonance. Thus it can be concluded the length of slot S_3 can be use to determine the second resonance.

Now it is known that the main determining factor of the second, third and fourth resonance is by the variation of the three slots' length. However, we have yet to investigate the effect when varying the short-circuit plate's width, which is an important characteristics seen in the single band PIFA. Thus an investigation on the variation of short circuit plate's width is carried out and the results are shown in the figure below (Figure 4.17).

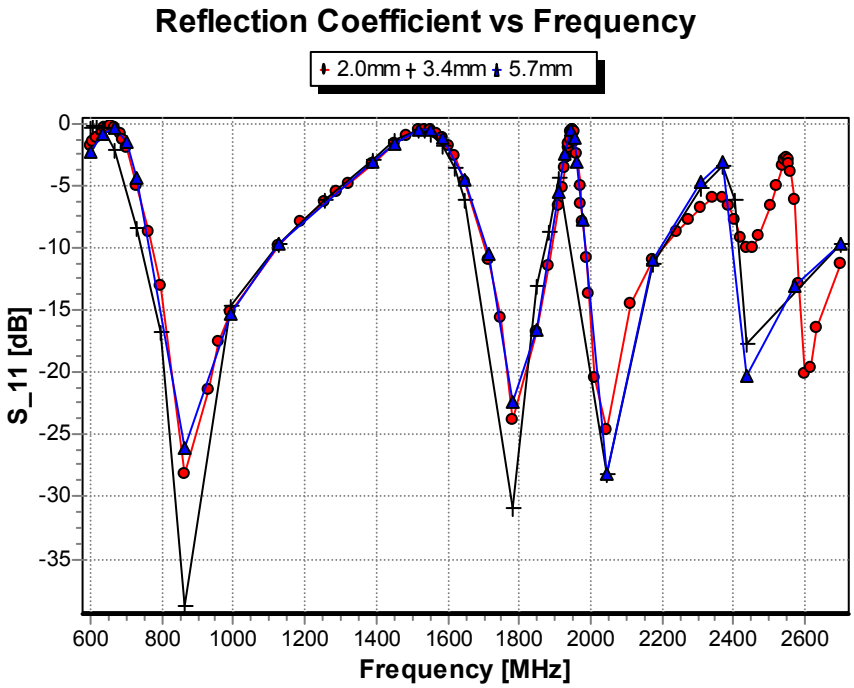

Figure 4.17: Return Loss Diagram for varying of short circuit plate's width

Figure 4.17 shows the return loss diagram with different short circuit plate's width. It can be seen that there is not much effect on the resonant frequencies. However, a slight shift on the fourth resonance can be noticed. In addition it can also be seen that there is an increase of bandwidth at the fourth resonance when the width increases. Therefore, after several experiments it was found that the best choice is when the width is 5.5mm.

Chapter 5

Results and Discussions

5.1 Introduction

The simulation software, FEKO, produced all the simulation results presented. All antenna designs were simulated and optimised over and over again till satisfactory results are obtained. Based on these results, discussions will be made on the performance of each antenna. In this chapter, the accomplished results such as return loss curves and radiation patterns will be discussed. In addition, analysis of the results of the quad band PIFA will be made to find out if it fulfils the basic criteria for operation in the proposed wireless communication networks or systems. Last but not least, a discussion will be made on the discovery of an extra resonant mode that in presence in the PIFA.

5.2 Single Band PIFA

Designing and simulating the 900MHz Planar Inverted-F Antenna using FEKO was the first step made in this thesis. As seen in the previous chapter, after a long and tedious process of simulation, the final structure and dimension of the antenna is shown in Figure 4.8. The following graph will show the return losses for the final antenna design.

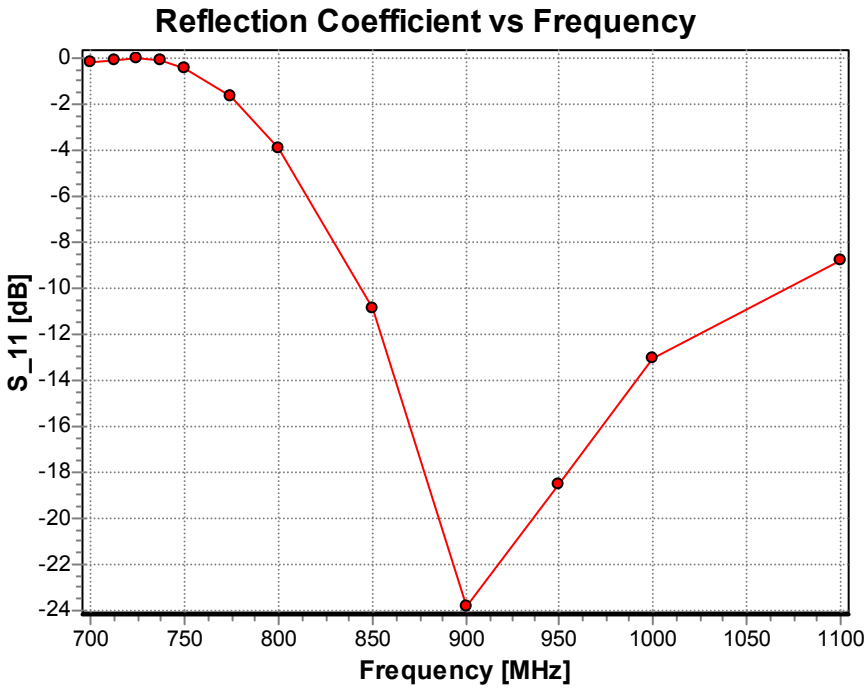

Figure 5.1: Simulated Return Loss for 900MHz PIFA

From the graph, Figure 5.1, it can be seen that a resonant frequency of 900MHz has been achieved. The return loss attain was approximated to be –24dB at 900MHz with bandwidth for S11≤ – 10dB of 225MHz (25.33%). It is located in the frequency range 844 – 1072MHz. The far-field radiation pattern of the antenna has also been measured. Figure 5.2 shows the distributions of the electric field, E_θ and E_Φ in the azimuthal plane (x-z plane).

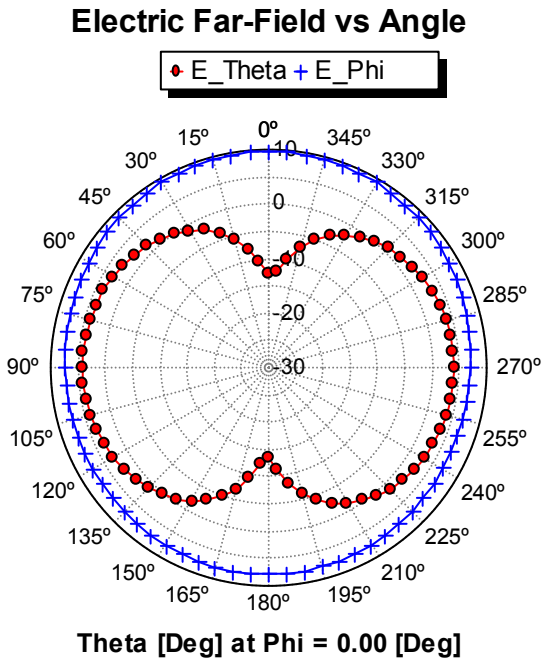

Figure 5.2: Radiation Pattern of the 900MHz PIFA in the x-z plane

For the radiation patterns in Figure 5.2, the E-Phi and E-Theta polarisations are examined. It can be seen that for the E-Phi field (vertical polarisation) more energy is radiated as compared to the E-Theta field. Also from the radiation pattern, the E-Theta field has a dip at $\theta = 0^{\circ}$ and 180°, which is probably due to the feed source that is shorted to the ground plane. Nevertheless, the radiation patterns are almost omnidirectional at all frequencies. Next discussion will be made on the results of the other three single-band PIFAs.

For 1800MHz:

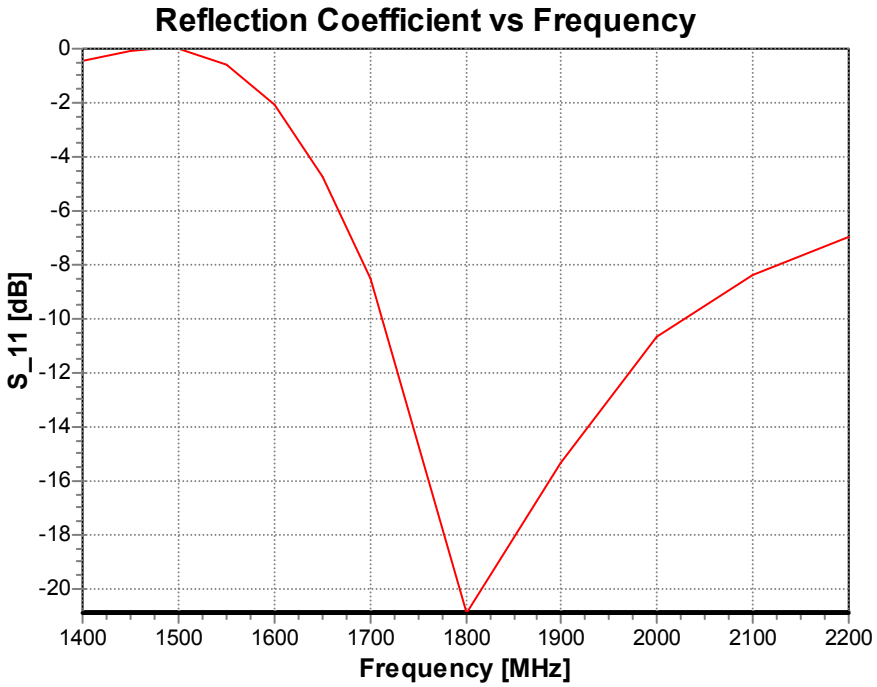

Figure 5.3: Simulated Return Loss for 1800MHz PIFA

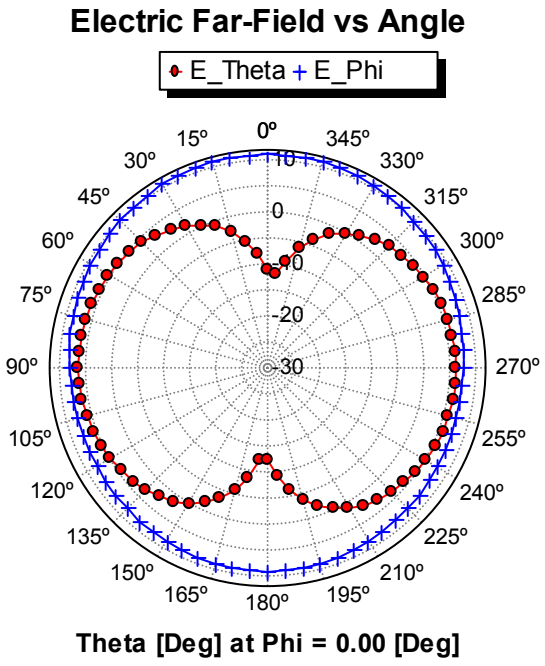

Figure 5.4: Radiation Pattern of the 1800MHz PIFA in the x-z plane

For 2GHz:

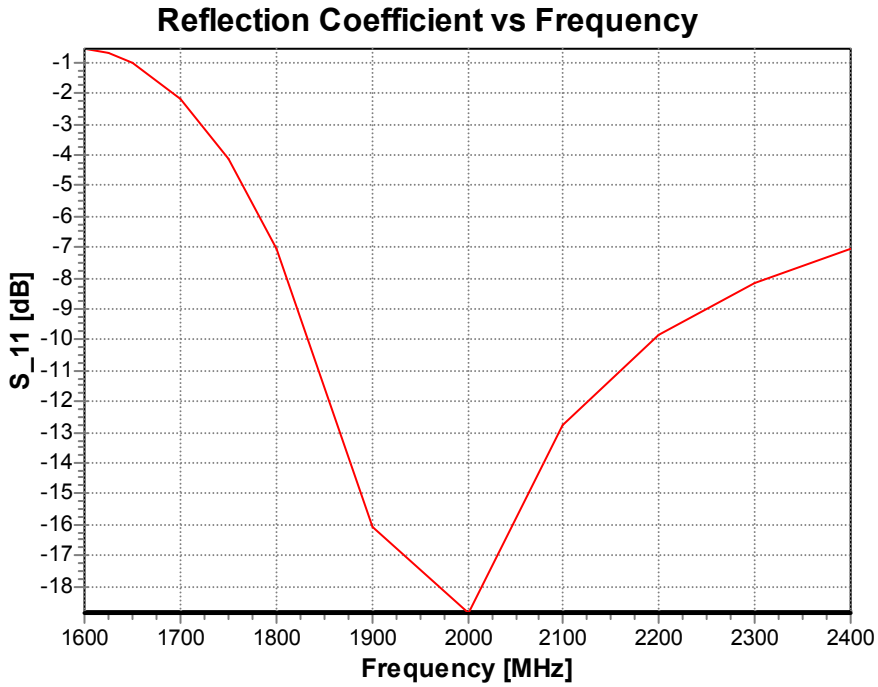

Figure 5.5: Simulated Return Loss for 2.0GHz PIFA

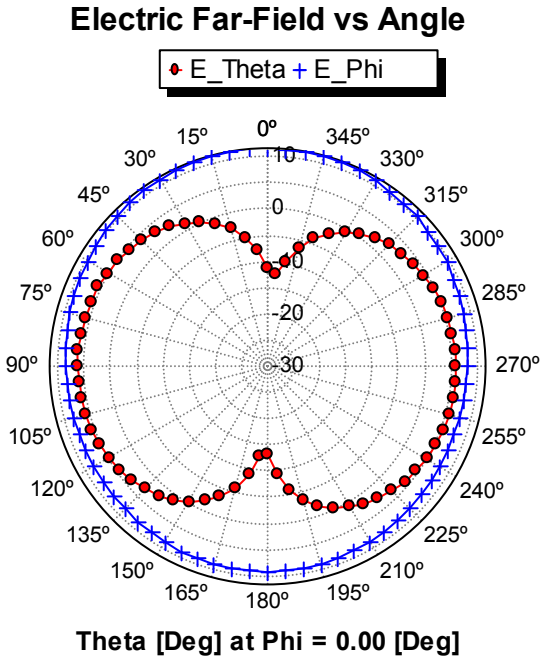

Figure 5.6: Radiation Pattern of the 2.0GHz PIFA in the x-z plane

For 2.4 GHz:

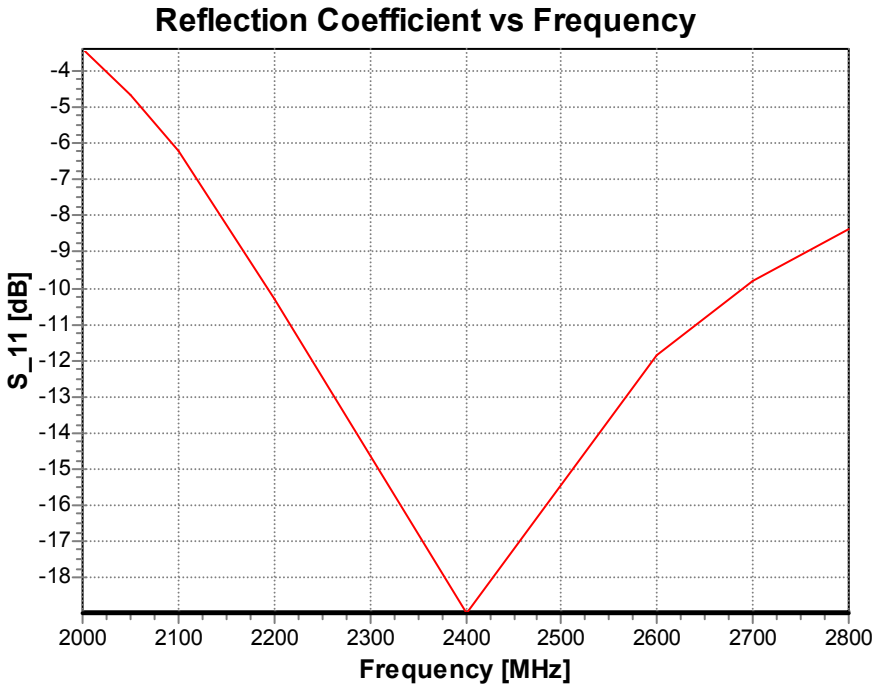

Figure 5.7: Simulated Return Loss for 2.4GHz PIFA

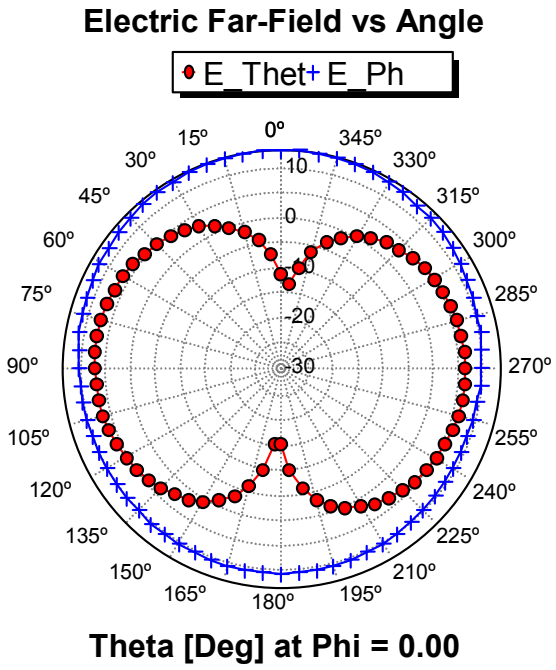

Figure 5.8: Radiation Pattern of the 2.4GHz PIFA in the x-z plane

From the results obtain for the three antennas, 1800MHz PIFA, 2.0GHz PIFA and 2.4GHz PIFA, it can be seen that the return loss for all the antenna are at least –18dB with bandwidths for S11≤ – 10dB of 342MHz (19%), 362MHz (18.1%) and 497MHz (20.7%) respectively. They are located in the frequency ranges of 1708 – 2050MHz for 1800MHz PIFA, 1833 – 2195MHz for 2.0GHz PIFA, and lastly 2193 – 2690MHz for 2.4GHz PIFA.

For the radiation patterns based on the graphs, Figure 5.3, 5.5, & 5.7, the E-Phi and E-Theta polarisations are examined. It can be seen that for all antennas E-Phi field (vertical polarisation) has more energy radiated as compared to the E-Theta field. Also from the radiation patterns, a dip at $\theta = 0^{\circ}$ and 180° can be seen in the E-Theta field. This dip in energy power is probably due to the feed source that is shorted to the ground plane. Nevertheless, these radiation patterns are almost omnidirectional at all frequencies.

5.3 Tri-Band PIFA

Based on the simulation performed using the design by Dou et al., a set of similar result is obtained. Figure 5.9 shows the return loss curve of the antenna with three resonant frequencies.

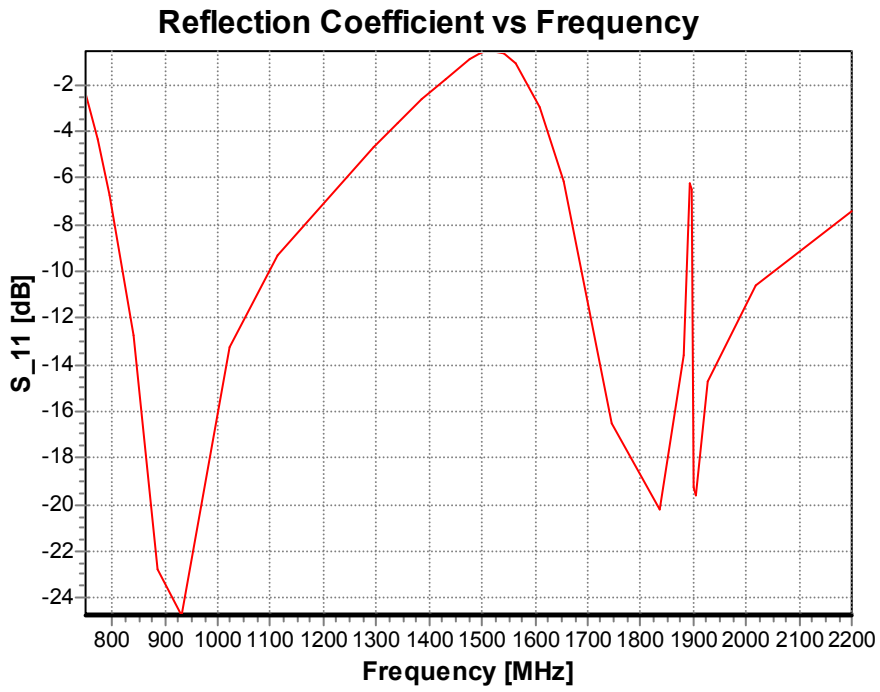

Figure 5.9: Simulated Return Loss for the tri-band PIFA by Dou et al.

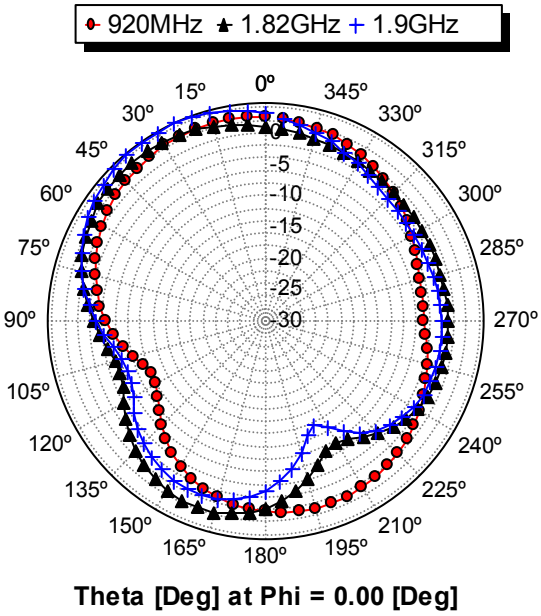

Figure 5.10: Radiation Pattern of the tri-band PIFA in the x-z plane

Form the radiation pattern in Figure 5.10, it can be clearly seen that the tri-band PIFA by Dou et al. is able to achieve an omnidirectional radiation pattern.

With the results from Figure 5.9 and 5.10, it can be concluded that this antenna is able to operate with three frequency bands, along with the good characteristics of a PIFA i.e. being small in size and able to have an omnidirectional radiation pattern.

5.4 Quad Band PIFA

Last of all, the main objective for this thesis is achieved thru the following results for the quad band PIFA. This set of optimised results is based on the design shown in Figure 4.13, which was simulated. The following graph will show the return losses for the final antenna design that produce four-frequency bands operation.

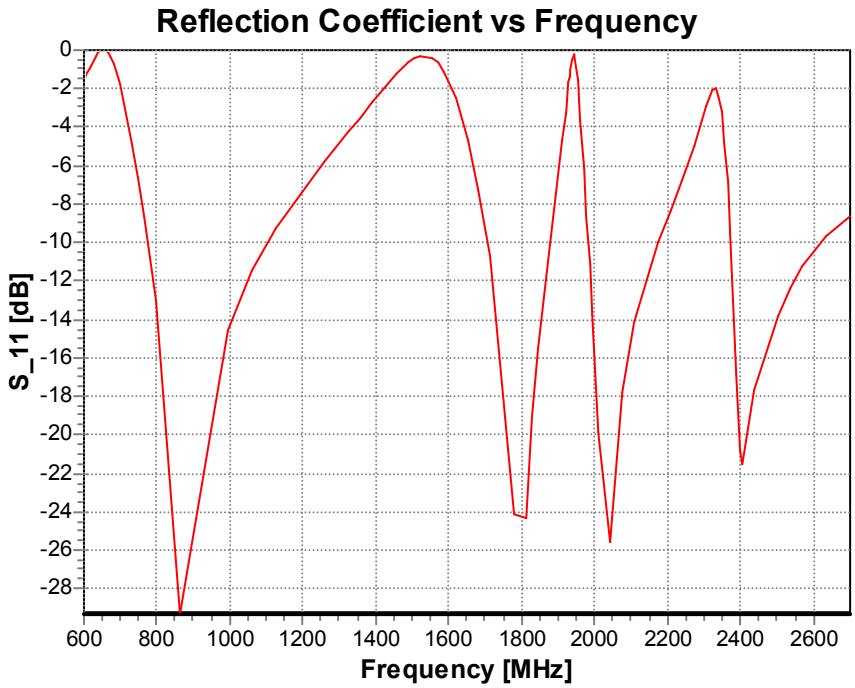

Figure 5.11: Simulated Return Loss for Quad Band PIFA

From this graph it can be observe that the four frequency bands are centred at 870MHZ, 1.8GHz, 2.04GHz and 2.4GHz, with bandwidths for S11≤ – 10dB of 329MHz (37.82%), 172MHz (9.56%), 192MHz (9.41%), and 247MHz (10.29%) respectively. They are located in the frequency ranges of 774 – 1103MHz for GSM900 operation, 1708 – 1880MHz for DCS1800 operation, 1983 – 2175 MHz for UMTS operation, and lastly 2373 – 2620MHz for Bluetooth operation.

The far-field radiation patterns for each frequency band of the quad band PIFA are obtained, and shown in Figure 5.12 is superimposed of four gain radiation patterns, in the azimuthal plane (x-z plane).

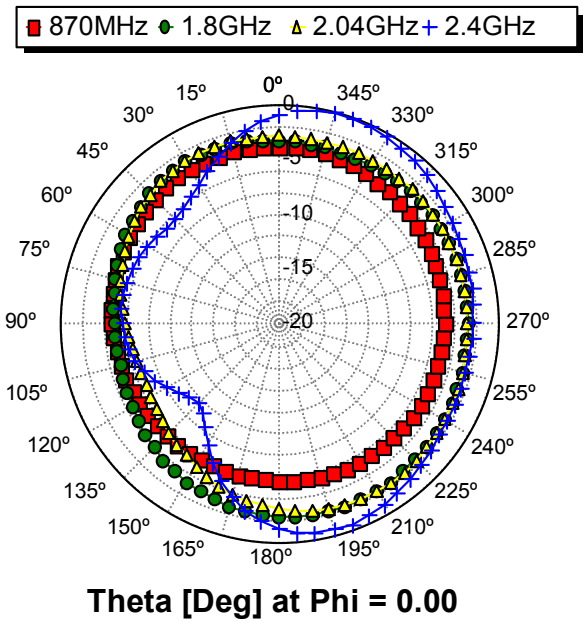

Figure 5.12: Far Field Gain of the Quad Band PIFA in the x-z plane

From the analysis of the graph, it can be seen from the four radiation patterns that generally, there is a higher gain towards the direction between $\theta = 0^{\circ}$ to 180°. The lower gain which is in the direction of $\theta = 90^{\circ}$ is believed to be cause by the three slots that are etched onto the antenna. It can also be observed that the gain on the left side of the graph for 1.8GHz, 2.04GHz and 2.4GHz gets lower as the frequency increase, which is probably due to the increase of slot length. Nevertheless, these radiation patterns are omnidirectional at all frequencies, which demonstrates that the antenna offers broad beamwidth for use on handheld transceivers.

The far-field radiation pattern for each frequency band of the quad band PIFA is also obtained, and shown in Figure 5.13, 5.14, 5.15 and 5.16 is the distribution of the electric field, E_{θ} and E_{Φ} in the azimuthal plane (x-z plane).

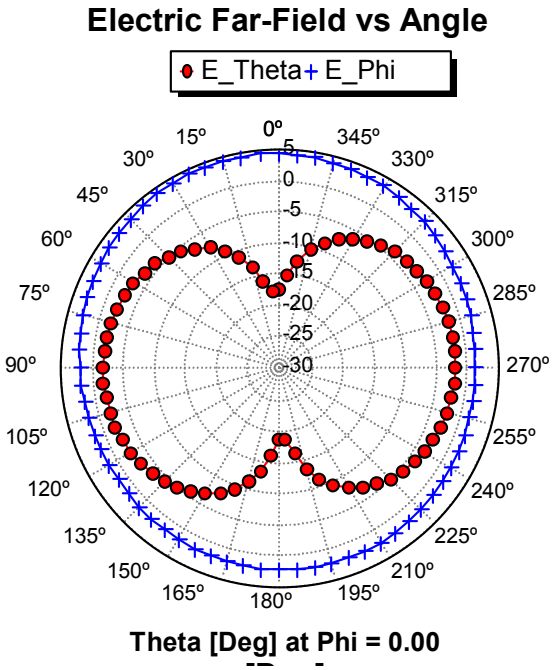

Figure 5.13: Radiation Pattern of the Quad Band PIFA at 870MHz in the x-z plane

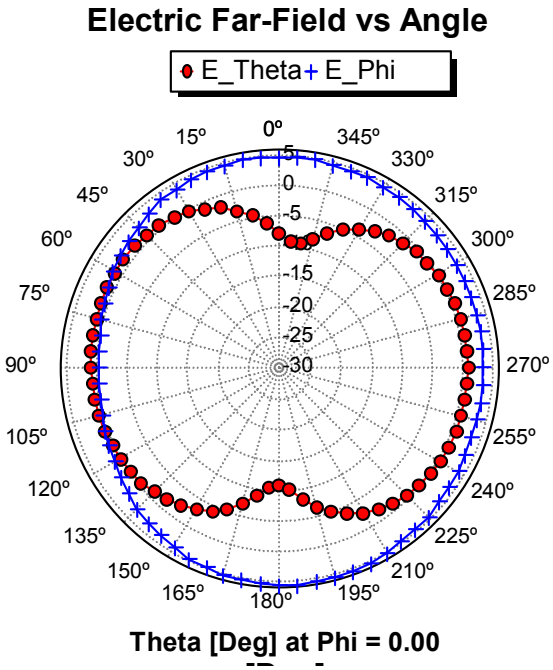

Figure 5.14: Radiation Pattern of the Quad Band PIFA at 1.8GHz in the x-z plane

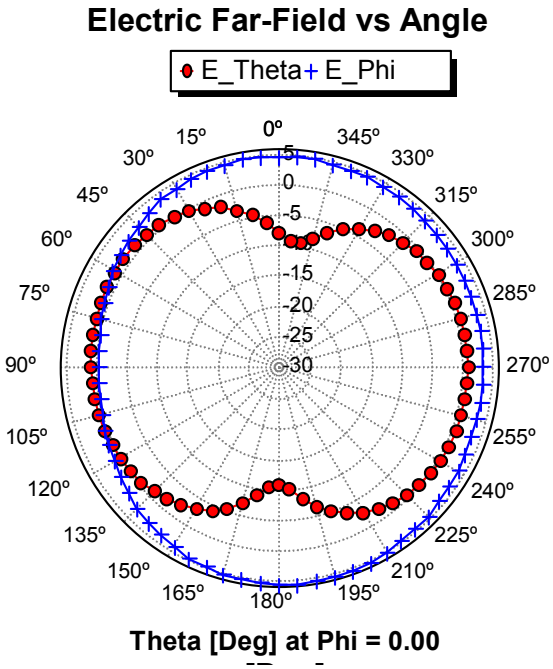

Figure 5.15: Radiation Pattern of the Quad Band PIFA at 2.04GHz in the x-z plane

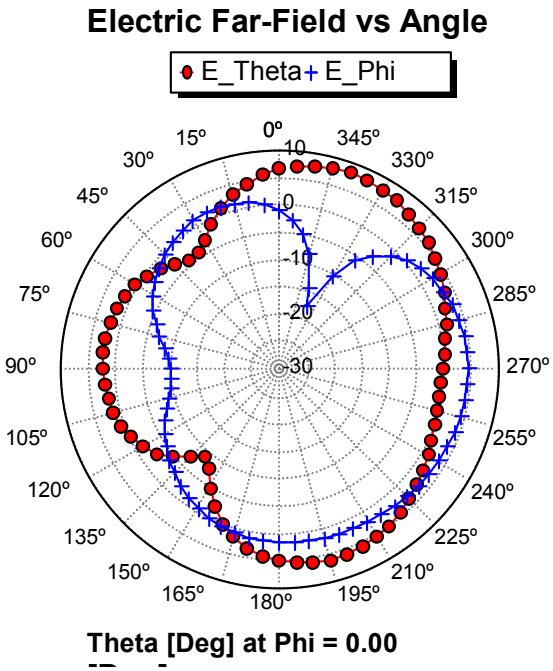

Figure 5.16: Radiation Pattern of the Quad Band PIFA at 2.4GHz in the x-z plane

Based on the four graphs (Figure 5.13, 5.14, 5.15 & 5.16), the E-Phi and E-Theta polarisations will be examined. It can be seen that for 870MHz, 1.8GHz and 2.04GHz the gain of the antenna is greatly influenced by the dominant E-Phi field (vertical polarisation). However for 2.4GHz the gain of the antenna is greatly influenced by the dominant E-Theta field (horizontal polarisation). Next from the radiation patterns a dip at around $\theta = 0^{\circ}$ and 180° can be seen this is probably due to the feed source which is shorted to the ground plane (same as what happened in the single band PIFA). Nevertheless, these radiation patterns are omnidirectional at all frequencies.

5.5 Extra Resonant Mode of the PIFA

It was seldom known to people that PIFA has an extra resonant mode. This extra resonant mode was discovered during the initial process antenna design and much confusion was caused. It can be seen from Figure 5.17, for a 900MHz PIFA, there is an extra resonant mode at around 3GHz. Nevertheless, this phenomenon was later found to be a characteristic of the Inverted-F Antenna (according to Reidy in [9]).

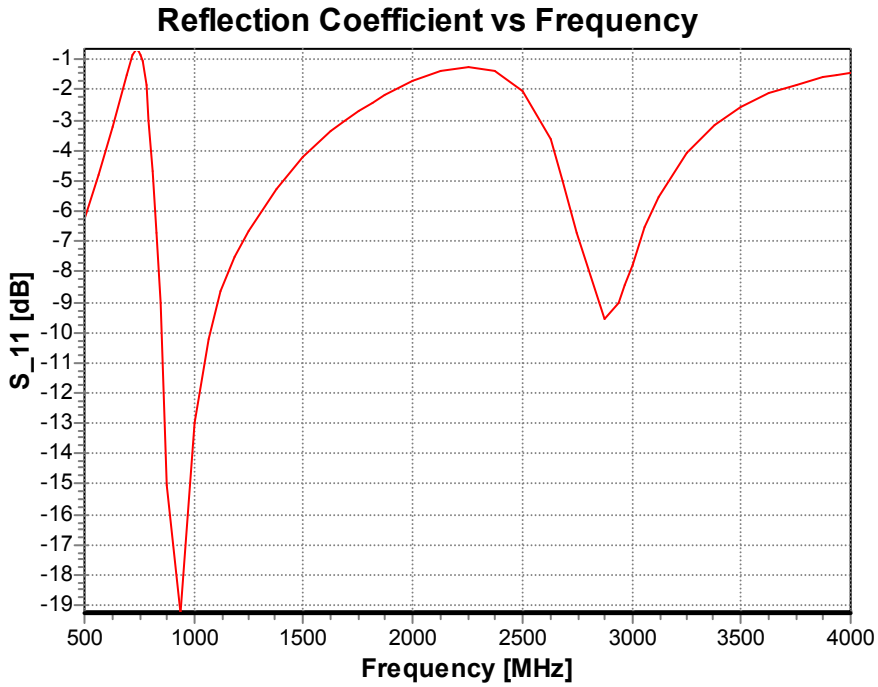

Figure 5.17: Return Loss Curve of the 900MHz PIFA with an extra resonant mode

Chapter 6

Conclusion and Future Work

During the last decade, the mobile radio communications industry has grew at an incredible rate. This phenomenon has not only seen a large increase of mobile phone subscribers worldwide but also produced more new communication systems. It is due to these reasons that the demand for multi-band antenna increases. With the advancement in technology, designs of portable communications devices such as mobile phones have now become smaller and more compact, thus requiring antenna to be small and low profile. Therefore, the purpose of this thesis is to design a multi-band antenna, for use on portable communications devices, which provides an embedded solution.

The main objective of this thesis is achieved with a new antenna designed that operates at 4 frequency bands. And it can be integrated with any handheld devices given its low profile and small size characteristics. However, this is done through a very complex and time-consuming process where problems were faced constantly. Nevertheless, many interesting characteristics of the antenna have been uncovered and flattering results are achieved.

Unfortunately, due to time constraint and lack of logistic support, further study on the quad band antenna needs to be carried out in order to prove that it is feasible, and can be used on a handheld transceiver. This includes the development of an antenna prototype to verify the characteristics and performance of the antenna, to study the performance of the antenna with human interaction and investigate the Specific Absorption Rate (SAR) distribution in a human model. Nevertheless, this thesis project is still deemed to be successful as most aspects of the Quad Band Planar Inverted-F Antenna had been examined and simulation results show that the antenna is suitable for use on a handheld

transceiver. Besides, it also has been shown that the simulation results obtained adhere to the theory.

There are a few conclusions that can be drawn from this thesis:

i) The designed multi-band antenna, built on PIFA design, is very sensitive to any changes to the dimension of the structure including the ground plane.

ii) The Spatial Network Method by Hirasawa et al. is very useful in understanding the main properties of PIFA.

iii) PIFA in general have two very good characteristics, which is small in size and having omnidirectional radiation pattern.

References

[1] T.S. Rappaport, "Wireless Communications, Principles & Practice", Prentice Hall, 2002

[2] K. Hirasawa & M. Haneishi, "Analysis, Design, and Measurement of Small and Low-Profile Antennas", Artech House, Inc, 1992

[3] Ya Jun Wang, Yeow Beng Gan, & Ching Kwang Lee, "A Broadband and Compact MSA IMT-2000, DECT, AND Bluetooth Integrated Handsets", Microwave and Optical Technology Letters, Vol. 32, No. 3, 2002

[4] Yong-Xin Guo, Kwai-Mun Luk, Kai-Fong Lee, & Ricky Chair, " A Quarter Wave U-Shaped Patch Antenna with Two Unequal Arms for Wideband and Dual Frequency Operation", 2001 IEEE Antennas & Propagation Society International Symposium, Vol. 4, pp. 54 – 57, 2001

[5] Z.D Liu, P.S Hall, & D Wake, "Dual Frequency Planar Inverted-F Antenna", IEEE Transactions on Antennas and Propagation, Volume 45, No.10, pp. 1451 – 1457, October 1997

[6] Shyh-Tirng Fang, & Jyh-wen Sheen, "A Planar Triple-Band Antenna for GSM/DCS/GPS Operations", 2001 IEEE Antennas & Propagation Society International Symposium, Volume 2, pp. 136 – 139, July 2001

[7] Eugene Borisov, & Thomas Moore, "A Quad-Band Stubby Antenna for Portable Wireless Devices", 2001 IEEE Antennas & Propagation Society International Symposium, Volume 4, pp. 542 – 544, 2001

[8] K. Fujimoto, A. Henderson, K. Hirasawa & J.R. James, "Small Antennas", Research Study Press, 1987

[9] Michael Reidy, “The Planar Inverted-F Antenna”, Thesis, University of Queensland, 1997

[10] Virga, K.L., & Rahmat – Sammi, “Low-profile enhanced-bandwidth PIFA antennas for wireless communications packaging”, IEEE Transactions on Microwave Theory Techniques, Volume 45, pp. 1879 – 1888, 1997

[11] Pekka Salonen, Lauri Sydänheimo, Mikko Keskilammi, & Markku Kivikoski, “A Small Planar Inverted-F Antenna for Wearable Applications”, Proceedings of the Third International Syposium on Wearable Computers, pp. 95 – 100, 1999

[12] Weiping Dou, & M.Y.W. Chia, “ E-shaped Planar Inverted-F Antenna with low-absorption for triple-band operation in cellular phones”, International Journal of Electronics, Volume 88, No. 5, pp. 575 – 585, 2001

APPENDIX

```
** Quad Band PIFA design program for use on FEKO

** Scaling factor (dimensions in mm)
SF   1                    0.001

** Parameters
#freq1 = 900.0e6
#lambda1 = #c0/#freq1*1000          ** Calculation of the wavelength
#freq2 = 1800.0e6
#lambda2 = #c0/#freq2*1000          ** Calculation of the wavelength
#freq3 = 2000.0e6
#lambda3 = #c0/#freq3*1000          ** Calculation of the wavelength
#diam = 1.3                         ** Diameter of the feeding probe
#tri_len = #lambda3/13
#seglen = #lambda3/13
#segrad = #diam/2

** Dimensions of PIFA
#Ly = 51.5-#Wd                      ** Length of the antenna (y-axis)
#Wx = 60.0                          ** Width of the antenna (x-axis)
#L1 = 23.6                          ** Length of slot 1
#L2 = 29.9                          ** Length of slot 2
#Wa = 23.9                          ** Width a
#Wc = 7.2                           ** Width c
#Wd = 13.0                          **Width d
#L3 = 33.35                         **Length of slot 3
#S3 = 2.0                           **Width of slot 3
#Ld = #Wd+#S3
#S1 = 2.0                           ** Width of Slot1
#S2 = #S1                           ** Width of Slot2
#G1 = 6.0                           ** Position of shorting strip 1
#G2 = 7.0                           ** Position of shorting strip 2
#F = -8.0                           ** Position of the feeding probe
#d = 5.5                            ** Width of the shorting strip
#h = 4.0                            ** Height of the PIFA
#Wb = #Ly-#Wa-#Wc-#S1-#S2           ** Width b

#GG1 = #G1+#d
#GG2 = #G2+#d
#GG3 = #G3+#d
#t = #Ly-#Wa
#m = #Wx/2              ** midpoint position


** Dimensions of ground
#a1 = #m+5                          ** X-axis
#a2 = 70                            ** Y-axis
```

```
** Define points for PIFA
IP                    #segrad   #tri_len  #seglen   5.0
** Define points for the foam
DP   F1               -#m       -#Wa      #h
DP   F2               #m        #t+#Ld    0
QU   F2   F1            1.02              0.0000001

** Define points for PIFA      X         Y        Z
DP   P1               -#m       -#Wa      #h
DP   P2               #F        -#Wa      #h
DP   P3               #m        -#Wa      #h
DP   P4               #m        0         #h
DP   P5               #L1-#m    0         #h
DP   P6               -#m       0         #h
DP   P7               -#m       #S1       #h
DP   P8               #L1-#m    #S1       #h
DP   P9               #m        #S1       #h
DP   P10              #m        #Wb+#S1   #h
DP   P11              #L2-#m    #Wb+#S1   #h
DP   P12              -#m       #Wb+#S1   #h
DP   P13              -#m       #Wb+#S1*2 #h
DP   P14              #L2-#m    #Wb+#S1*2 #h
DP   P15              #m        #Wb+#S1*2 #h
DP   P16              #m        #Ly-#Wa   #h
DP   P17              #L2-#m    #Ly-#Wa   #h
DP   P18              -#m       #Ly-#Wa   #h

**Add on
DP   A1               -#m       #t+#S3    #h
DP   A2               #L2-#m    #t+#S3    #h
DP   A3               #m        #t+#S3    #h
DP   A4               #m        #t+#Ld    #h
DP   A5               #L2-#m    #t+#Ld    #h
DP   A6               -#m       #t+#Ld    #h
DP   A7               #L3-#m    #t+#S3    #h
DP   A8               #L3-#m    #Ly-#Wa   #h


** Define point for shorting strips
DP   P21              #m        -#Wa+#G2  #h
DP   P22              #m        -#Wa+#GG2 #h
DP   P23              #m        -#Wa+#GG2 0
DP   P24              #m        -#Wa+#G2  0
DP   P31              #m-#G1    -#Wa      #h
DP   P32              #m-#GG1   -#Wa      #h
DP   P33              #m-#GG1   -#Wa      0
DP   P34              #m-#G1    -#Wa      0
```

```
DP   P51                #m-#G3    #t+#Ld    #h
DP   P52                #m-#GG3   #t+#Ld    #h
DP   P53                #m-#GG3   #t+#Ld    0
DP   P54                #m-#G3    #t+#Ld    0


** Generated the PIFA
LA    1
PM   P31  P32  P3   P21      P22      P4       P5       P6       P1       P2
BP   P9   P8   P5   P4
BQ   P11  P12  P7   P8
BQ   P10  P11  P8   P9
BP   P15  P14  P11  P10
PM   P13  P14  P15  P16      P17      A8       P18
PM   A1   A7   A2   A3       A4       P51      P52      A5       A6
PM   A8   A7   A2   A3       P16      P17


** Generated the Shorting strips
LA    2
BP   P21  P24  P23  P22
BP   P31  P32  P33  P34


** Define point for Gound plane
DP   P41                #a1      #a2      0
DP   P42                #a1      -#Wa     0
DP   P43                -#a1     -#Wa     0
DP   P44                -#a1     #a2      0


** Define segment for the feeding probe
** Define axis             X        Y        Z
DP   S1                 #F       -#Wa     #h
DP   S2                 #F       -#Wa     0

** Define label for the feeding probe
LA    3
BL    S2   S1

** Generate the Ground Plane
LA   0
PM   P41  P44  P43  S2       P33      P34      P42


** End of the geometry input
EG   0    0    0    0    0
PS        0    0    1    0
```

```
** Load the feed segment with 50ohm impedance
LZ   3                    50

** Excitation
FR   200  2                600e6             2700e6
A1   0    3                1         0
PW   1    0                1.0

** Calculates the far field in 2 vertical planes
FF   1    72   72   1         0.0       0.0       5.0       5.0

** Calculates the electric & magnetic near fields along the x axis
FE   7

EN
** End
```